Politecnico di Milano

Modeling the Covid-19 epidemic: Theoretical and experimental assessments

Supervisor

Silvia Lorenzani

Co-Supervisors

Stefano Finazzi

Marzia Bisi

Candidate

Matilde Perego – 10482750

To my grandmother,

Liberina

Ringraziamenti

Un sentito ringraziamento alla Professoressa Silvia Lorenzani, mia relatrice, non solo per avermi guidata in questo percorso, ma soprattutto per avermi trasmesso la sua passione e la voglia di scoprire cose nuove.

Ringrazio Stefano Finazzi, il mio tutor, per avermi fatto affacciare in un mondo che non conoscevo spiegandomi ogni cosa con pazienza.

Ringrazio la Professoressa Marzia Bisi, co-relatrice di questa tesi.

Ringrazio i Phorkoni, compagni di sventure, che hanno reso l'ultimo anno più bello.

Ringrazio di cuore a tutte le mie amiche, Margherita, Cecilia, Bianca e le pazzeskeh Unikorne per essermi sempre state vicine in questo percorso facendomi distrarre (anche troppo), supportandomi nei momenti difficili e strappandomi sempre un sorriso. Se non fosse per loro avrei perso anche quel briciolo di sanità mentale che mi è rimasto.

Infine, ultima ma non ultima, ringrazio la mia famiglia, che dall'inizio di questo percorso mi è sempre stata vicina e mi ha sempre spronata ad andare avanti "come un panzer".

Contents

Abstract

Lo scopo del presente studio è duplice. In primo luogo abbiamo derivato un modello microscopico per la diffusione su larga scala del virus SARS-CoV-2 attraverso un approccio di Meccanica Statistica. In secondo luogo abbiamo cercato di capire come dei microrganismi infettivi, le Enterobacteriaceae resistenti ai carbapenemi (CRE), possano diffondersi tra i pazienti dei reparti di terapia intensiva (TI), peggiorando le loro condizioni di salute. Questo studio è stato svolto in collaborazione con l'Istituto per la Ricerca Farmacologica Mario Negri. Poiché lo stesso problema emerge con il Covid-19 e il modello proposto per il parametro di trasmissione delle Enterobacteriaceae resistenti ai carbapenemi in terapia intensiva è governato dalle stesse leggi probabilistiche alla base dell'evoluzione della pandemia di Covid-19, abbiamo potuto tracciare un parallelismo tra CRE e SARS-CoV-2. Dopo l'elaborazione e l'analisi dei dati, abbiamo valutato il parametro di trasmissione β, presente anche nei modelli epidemiologici, e attraverso il metodo Monte Carlo abbiamo determinato il relativo intervallo di confidenza.

Dopo un'introduzione presentata nel Capitolo 1, il Capitolo 2 contiene una panoramica dei modelli epidemiologici compartimentali esistenti in letteratura, mentre il Capitolo 3 fornisce una breve descrizione della malattia Covid-19 e in particolare della risposta del sistema immunitario. Il Capitolo 4 è dedicato alla presentazione di alcuni aspetti della teoria cinetica (legati all'equazione di Boltzmann) che sono stati sfruttati per derivare il nostro modello, presentato in dettaglio nel Capitolo 5. L'idea innovativa alla base della derivazione del modello si basa sul seguente presupposto: il contagio avviene non solo per contatto diretto ma anche a distanza. Ciò giustifica l'uso di un "potenziale di interazione" tra individui per descrivere la diffusione dell'epidemia.

Abstract

The aim of the present study is twofold. Firstly we have derived a microscopic model for the large-scale spread of SARS-CoV-2 virus through a Statistical Mechanics approach. Secondly we have tried to understand how an infectious microorganism, the carbapenem-resistant Enterobacteriaceae (CRE), can spread among patients in intensive care units (ICUs), worsening their health conditions. This part has been carried out in collaboration with the Mario Negri Institute for Pharmacological Research. Since the same problem arise with Covid-19 and the model proposed for the transmission parameter of Carbapenem-resistant Enterobacterales in ICUs is governed by the same probabilistic laws at the basis of the dynamics of outbreaks of infectious diseases such as the Covid-19 pandemic, we have drawn a parallelism between CRE and SARS-CoV-2. After processing and analyzing the data, we have evaluated the transmission parameter β, also present in epidemiological models, and through the Monte Carlo method we have determined the relative confidence interval.

After an introduction presented in Chapter 1, Chapter 2 contains an overview of compartmental epidemiological models existing in the literature, while Chapter 3 provides a brief description of Covid-19 disease and in particular of the response of the immune system. Chapter 4 is devoted to the presentation of some aspects of the kinetic theory (related to the Boltzmann equation) that have been exploited to derive our model, presented in detail in Chapter 5. The innovative idea behind the derivation of the model relies on the following assumption: contagion occurs not only through a direct contact but also at a distance. This justify the use of an "interaction potential" between individuals to describe the spread of infection.

Chapter 1

Introduction

Since the beginning of the last century, a large number of mathematical models have been developed to predict on a large scale the dynamics of the spread of epidemics in the population [1]. However, due to the complexity and intrinsic stochasticity of the phenomenon to be described, most of the available models are only qualitative and cannot capture the details of the epidemic spread. In this framework, among the most widely used models one can include those of SIR-type (in which the population is divided in compartments, in accordance to the state of individual health, such as susceptible (S), infected (I) and recovered (R)) or SIS (in which a recovered individual returns immediately to be susceptible) [2]. This class of models describes, under the mean-field approximation, the temporal evolution of the average number of susceptible, infected and recovered individuals, through systems of ordinary differential equations. Here the following appear as parameter: the disease transmission probability, the probability that an infected individual recovers, the average length of the period in which an individual can transmit the infection. The parameters that appear in the SIR or SIS models are empirically estimated on the basis of the available data related to past epidemics. And it is precisely the phenomenological and non-self-consistent nature of these models that represent their greatest weak point. This negative aspect arose predominantly in the recent health-emergency due to the spread of SARS-CoV-2 virus. Although the epidemiological models present in the literature have been useful tools to be able to predict epidemic diffusion scenarios, especially in relation to the various containment measures put in

place by governments, none of them has been able to quantitatively describe the real transmission of the virus (nor as regards the incidence, in terms of number of cases, nor as regards the evaluation of a 'peak' of the epidemic, intended as a stationary state of the model). The primary objective of the proposed research project is to improve the existing mathematical models using the tools of Statistical Mechanics of complex systems. Following this type of approach, it is possible to determine the mechanism of transmission on a large scale starting from a microscopic modeling of the interactions between individuals. The reference mathematical setting is that of the kinetic theory and the Boltzmann equation, originally derived to model the macroscopic properties of rarefied gases through the microscopic analysis of molecular interactions [3].

In recent decades, there have been several reformulations of the non-equilibrium Statistical Mechanics, described by Boltzmann-like equations, for applications in the field of Life Sciences [4]. In this framework, a possible scenario for the construction of epidemiological models has been also developed, which, however, in the absence of an application need, remained at an embryonic level. Therefore, the primary aim of the proposed research project is that of the theoretical formulation and numerical implementation of a self-consistent mathematical model, able to quantitatively describe the evolution of an epidemic, while providing for the possibility of stopping its spread. The project is divided into the following steps:

(a) The derivation of a system of integro-differential equations that describes the spatio-temporal evolution of the distribution functions of groups of individuals (susceptible and infected) starting from the form of the Boltzmann equation for gas mixtures. In the framework of the present project, each component of the mixture represents a group of individuals, characterized by a distribution function dependent on a microscopic variable that describes their state (as the molecular velocity in the case of gas mixtures). This variable is called *activity* and allows to identify healthy, positive asymptomatic, positive symptomatic and hospitalized individuals among the two main classes of susceptible and infected. The integral term of this system of Boltzmann-like equations describes the interaction between individuals, belonging to the same group or to

different groups, determining the change in the microscopic state of each of them. Also in this case, the modeling of the integral term takes place in close analogy with what is usually done for gas mixtures, i.e. assuming an 'interaction potential'. This is the most innovative aspect of the proposed model, which makes it self-consistent and also allows one to include the peculiarities of spread of SARS-CoV-2 virus, as it provides the possibility of inserting long-range 'interaction potentials' between individuals (as usually happens for interactions between the molecules of a gas) while, for example, in SIR or SIS type models, it is assumed that the infection occurs by direct contact. The transition from a group to another is described through the law that governs the reactive gas mixtures i.e. chemically active gas, that changes its properties in different atmospheres and can even react with the materials it comes into contact with. The probability to change state or class due to the interaction of individual immune system is represented by a linear term. Here both the innate and adaptive immune system is taken into consideration according to the data related of the evolution of antibodies as a result of SARS-CoV-2 contagion [5] (see Sec. (3.0.2)).

By averaging the distribution functions of the various groups of individuals, with respect to the microscopic variable associated with them, it is possible to derive a macroscopic model that provides the temporal evolution of the average number of individuals belonging to each group. The comparison with the real epidemiological data can allow to identify the most suitable 'interaction potential' to describe a given epidemic, in such a way as to be able to predict its evolution. At the same time, the analysis of different models of interaction between groups of individuals can provide the opportunity to study the effectiveness of social distancing measures.

(b) In general, determining the numerical solution of a system of Boltzmann-like equations is a complex problem, since it requires knowledge of specific integration tools in the field of Statistical Mechanics. In order to develop a model that can be used by a wide range of users, which allows rapid forecasting in a context of health-emergency but which, at the same time, retains the

peculiarity of a microscopic derivation (as illustrated in (a)).

The project involves the following units:

(*) The Department of Mathematics, Politecnico di Milano, with Silvia Lorenzani (Associate Professor, principal investigator);

(**) The Department of Mathematical, Physical and Computer Sciences, University of Parma, with Marzia Bisi (Associate Professor);

(***) The Pharmacological Research Institute Mario Negri (IRCCS), with the researcher Stefano Finazzi.

Chapter 2

Epidemiological models

2.1 Overview of epidemiological models

Epidemic dynamics is an important method of studying the spread of infectious disease qualitatively and quantitatively. It is based on the specific property of population growth, on the spread rules of infectious diseases and on the related social factors.

Mathematical epidemiology modeling has grown exponentially starting in the middle of the 20th century (in particular in 1957 with Bailey's book [9]) and from that moment on a large variety of models have now been formulated, mathematically analyzed and applied to infectious diseases. This study became so relevant to be part of epidemiology policy decision making in many countries, which accounted on mathematical modeling in order to build a public health policy in response to diseases such as gonorrhea, HIV/AIDS, BSE, foot and mouth disease, measles, rubella, and pertussis. Understanding the transmission characteristics of infectious diseases in communities can in fact lead to better approaches to decrease the transmission of these illness. Decision-making based on epidemiological models became more and more found of also thanks to the introduction of deterministic and/or stochastic models, computer simulations, Monte Carlo models, microsimulations of individuals in a community and small world and other network models.

The model formulation process has to clarify assumptions, variables and parame-

ters. Moreover it provides conceptual results such as thresholds, basic reproduction
or contact numbers. All of these are useful experimental tools for building and
testing theories, assessing quantitative conjectures, answering specific questions, de-
termining sensitivities to changes in parameter values and estimating key parameters
from data. Epidemiology in fact not only describe the distribution of the disease
but it also allows to identify the causes or risk factors, to design and test theories, to
evaluate detection, control and prevention programs and to make general forecasts.

Epidemiologists and policy makers need to be aware of both the strengths and
weaknesses of the epidemiological modeling approach. Epidemiological models start
in fact from a microscopic description of reality (interactions between single individ-
uals) to predict the macroscopic behavior of disease spread through a population.
The difficulty lies in the fact that transmission interactions in a population very
complex, so that it is difficult to comprehend the large scale dynamics of disease
spread without the formal structure of a mathematical model.
The first and most evident limitation is that all epidemiological models are simpli-
fications of reality (for example, it is often assumed that the population is uniform
and homogeneous) and this deviation from reality is scarcely testable or measurable.
People in fact do not behave in reasonably predictable ways like molecules, cells or
particles. Because of this reason one can never be completely certain about the
validity of results obtained and sometimes questions cannot be answered by using
epidemiological theory.

However an advantage of mathematical modeling is the clarity and precision of
the mathematical formulation: any model using integral or differential equations is
not ambiguous or vague. Of course, the parameters must be defined precisely and
each term in the equations must be thoroughly explained in terms of mechanisms,
but the resulting model is a definitive statement of the basic principles involved.
In order to choose and use epidemiological modeling effectively, one must understand
the behavior of the specific disease and be acquainted with the available formulations
and all the implications of choosing a particular formulation rather than another.
Once the formulation is complete, threshold, equilibrium, periodic solutions and

their local or global stability can be determined with different mathematical techniques.

Both deterministic or stochastic models are used. Deterministic models use integral or differential equations to describe the changes in time of the sizes of the epidemiological classes, according to which, given the initial condition for a well-posed deterministic model, the solution is unique. Stochastic models apply probabilities at each time step to determine any movement from one epidemiological class to another. When these models are simulated the probabilities are calculated using random number generators or distributions, so that the outcomes of different runs are different and these approaches are called Monte Carlo simulations, which we will exploit in *Chapter 5*. Conclusions are obtained by averaging the results of a large enough number of simulations.

Deterministic models do not reflect the role of chance in disease spread, whereas stochastic models incorporate chance, but it is usually harder to get analytic results for these models.

Recent models have involved aspects such as herd or disease-acquired immunity, stages of infection, vertical transmission, age structure, social and sexual mixing groups, spatial spread, quarantine and vaccination and its gradual loss. When formulating a model for a particular disease, it is necessary to decide which factors to include and which to omit. This choice often depends on the particular question that is to be answered.

Simple models have the advantage that there are only a few parameters, but they have the disadvantage of possibly being naive and unrealistic. Complex models may be more realistic, but they may contain many parameters for which value estimates cannot be obtained. The aim of epidemiological modeling is to make suitable choices in the model formulation so that it is as simple as possible and yet it is adequate for answering the question being considered and producing attainable results.

2.2   Compartmental models

Epidemiological modeling refers to dynamic system according to which population is divided into compartments based on their epidemiological status (e.g. susceptible, infectious, recovered...). Transition between compartments is described deterministically by differential and/or integral equations.

The most popular epidemic dynamic models are the so called *compartmental models* which were constructed by Kermack and Mckendrick in 1927 [10] and have been developed further by many other bio-mathematicians.

2.2.1   Formulation of the model

Compartments: S, I, R, E, M

In compartmental models the population under consideration is divided into disjoint classes whose sizes change with time t.

In the basic epidemiological models presented in this chapter, it is assumed that the population has constant size N. It means that a conservation law for the population size can be stated:

$$\sum_{i=1}^{N_c} C_i(t) = N \tag{2.1}$$

where N_c is the number of compartments of the model and C_i is the size of the i-th class at time t. N is assumed to be sufficiently large so that the sizes of each class $(S(t),\ I(t),\ R(t),\ E(t),\ M(t),\ ...)$ can be considered as continuous variables. Conservation of population size is achievable whether the disease spreads in a closed environment with no emigration or immigration, and no births or deaths, or whether vital dynamics are considered. In this last case, these phenomena should occur at equal rate. As an example let consider a model in which births and deaths are taken into consideration: let μ be the birth/death rate, if we assume that both susceptibles and infected can give birth then μN corresponds to the number of newborns per unit time, while $-\mu S(t)$ and $-\mu I(t)$ correspond to the deaths of susceptible and infected

individuals respectively so that

$$\mu N - \mu S - \mu I = \mu N - \mu(S + I) = \mu N - \mu N = 0. \qquad (2.2)$$

Basic models assume that the population is homogeneously mixing.

The most known classes in the literature are the following.

- The **susceptible compartment** $S(t)$, in which all individuals can contract the disease.

- The **infected compartment** $I(t)$, in which all individuals are infected and can infect other people.

- The **recovered compartment** $R(t)$, in which all individuals that heal from disease converge if the disease involves immunity. It means they cannot be infected again permanently or just temporarily, according to the disease features.

- The **exposed compartment** $E(t)$, in which individuals are infected, but not yet infectious i.e. whose are in the latent period. After the latent period ends, the individual enters the class $I(t)$ of infectives and becomes capable of transmitting the infection.

- The **passive immunity compartment** $M(t)$, in which individuals are infants with passive immunity. They represent the newborns whose mother has been infected and some antibodies have been transferred across the placenta, so that the infant has temporary passive immunity to an infection. After the maternal antibodies disappear from the body, the infant moves to the susceptible class $S(t)$. Infants who do not have any passive immunity, because their mothers were never infected, directly enter the class $S(t)$ of susceptible individuals.

The choice regarding which compartments to include in a model depends on the characteristics of the particular disease being modeled and the purpose of the model. Some among the more common models are: SI, SIS, SIR, SIRS, SEI, SEIS, SEIR, SEIRS, MSEIR, and MSEIRS.

Incidence function

The horizontal incidence is the infection rate of susceptible individuals through their contacts with infectives, i.e. it is the number of new cases per unit time. Most of the forms for incidence functions involve S, I and N so that $f_{incidence} = f(S,I,N)$. Let β be *contact rate* i.e. the average number of adequate contacts of a person per unit time. For sexually transmitted diseases, it is useful to define both a sexual contact rate and the fraction of contacts that result in transmission. Instead for directly-transmitted diseases they are replaced by a definition that includes both since there is no clear definition of contact or transmission fraction, as they spread primarily by aerosol droplets and by transmission that may occur by entering a room, hallway, building, etc. which is currently or has been occupied by an infective. An adequate contact is a contact that is sufficient for transmission of infection from an infective to a susceptible.

We introduce the susceptible and infectious fractions, $s(t) = \dfrac{S(t)}{N}$ and $i(t) = \dfrac{I(t)}{N}$, where $S(t)$ and $I(t)$ are the number of susceptibles or infectives at time t, respectively. The most popular forms of incidence functions are the following two.

- *Standard incidence*:

$$f_{si}(S, I, N) = \beta\, S(t) I(t) / N = \beta\, s(t)\,(i(t) N) \tag{2.3}$$

  where $\beta \dfrac{S(t)}{N}$ is the average number of contacts with susceptibles per unit time of one infective, that has been multiplied by the number of infected individuals to obtain the number of new cases per unit time. Here we assume that the contact rate β is fixed and does not depend on the population size N or vary seasonally.

- *Mass-law action*:

$$f_{mla}(S, I, N) = \eta\, S(t) I(t) = \eta\,(N s(t\,(i(t) N) \tag{2.4}$$

  where the parameter η has no direct epidemiological interpretation, but comparing it with the standard formulation shows that $\beta = \eta N$, so that this form implicitly assumes that the average contact number β increases linearly

with the population size. Naively, it might seem plausible that the population density and hence the contact rate would increase with population size, but the daily contact patterns of people are often similar in large and small communities, cities, and regions. For human diseases the contact rate seems to be only very weakly dependent on the population size.

Incidence functions have the typical form

$$f(S, I, N) \ = \ \eta \, N^v \, \frac{S(t) \, I(t)}{N} \tag{2.5}$$

and data for five human diseases in communities with population sizes from 1,000 to 400,000 ([11] [12]) implies that v lies between 0.03 and 0.07. This strongly suggests that the standard incidence corresponding to $v = 0$ is more realistic for human diseases than the simple mass action incidence corresponding to $v = 1$. This result is consistent with the concept that people are infected through their daily encounters and the patterns of daily encounters are largely independent of community size within a given country (e.g. students of the same age in a country usually have a similar number of daily contacts). Thus the incidence function form that we will use in the next sections to present some example of the most popular compartmental models is the standard incidence function defined in (2.3).

Vertical incidence corresponds to the infection rate of newborns caused by their mothers. Sometimes it is included in epidemiological models by assuming that a fixed fraction of the newborns are infected vertically, but we will not take it into consideration.

Transfer rates between compartments

A common assumption is that the transfer rates between compartments are expressed mathematically as derivatives with respect to time of the sizes of the compartments. It has been shown [13] that these terms correspond to exponentially distributed waiting times in the compartments or, another possible assumption is that the fraction still in the compartment t units after entering is a non-increasing, piecewise continuous function $P(t)$ with $P(0) = 1$ and $P(\infty) = 0$. Transitions between classes are though governed by terms like δM, εE, γI, where

- δ is the passive-immunity loss rate. It corresponds to the transfer rate of newborns from passive immune class whom, at the end of an average period of $1/\delta$ units of time, lose their immunity and enter the susceptible compartment;

- ε is the latency loss rate. It corresponds to the transfer rate of individuals from exposed class to infected compartment since, after an average period of $1/\varepsilon$ units of time, an exposed becomes infective;

- γ is the recovery rate of infected individual whom recovers after a mean of $1/\gamma$ units of time and come back to the susceptible or recovered class, according to the fact disease entails immunity or not.

Take as example the transfer dynamics γI. It corresponds to $P(t) = e^{-\gamma t}$ as the fraction of individuals that are still in the infective class t units after entering this class because they became infective, with $1/\gamma$ as the mean waiting time. The rate at which individuals leave the compartment $I(t)$ at time t is $-\dot{P}(t)$ so, exploiting integration by parts, the mean waiting time in the compartment is

$$\int_0^\infty t\,(-\dot{P}(t))dt = \int_0^\infty P(t)\,dt = \int_0^\infty e^{-\gamma t}\,dt = \left[-\frac{e^{-\gamma t}}{\gamma} \right]_0^\infty = \frac{1}{\gamma}$$

The same exponential behaviour and thus results hold for the other rates δ and ε.

Birth and death rates are usually taken into consideration according to the kind of infection we are considering. An epidemic is an unusually large, short term outbreak of a disease, while a disease is called endemic if it persists in a population. Thus epidemic models are used to describe rapid outbreaks that occur in less than one year, while endemic models are used for studying diseases over longer periods, during which there is a renewal of susceptibles by births or recovery from temporary immunity and natural deaths.

The spread of an infectious disease involves not only disease-related factors such as the infectious agent, mode of transmission, latent period, infectious period, susceptibility and resistance, but also social, cultural, demographic, economic and geographic factors.

2.2.2 Thresholds: R_0, σ and R

There are three quantities that are important to take into consideration since their value are indicators of the spread of the disease.

The first one is the *basic reproduction number R_0* representing the average number of secondary infections that occur when one infected individual is introduced into a completely susceptible host population. R_0 is only defined at the time of invasion and it is often used as the threshold quantity which determines whether a disease can invade a population and become endemic or not.

The *contact number σ* is defined as the average number of adequate contacts of an infective individual during the infectious period. We remember that for "adequate" contact we intend an interaction that is sufficient for transmission of the disease when an infected meets a susceptible.

The *replacement number R* is defined to be the average number of secondary infections produced by a typical infective during the entire period of infectiousness at time t. Thus it is function of time and changes as the disease evolves.

At the beginning of the spread these three quantities, R_0, σ and R, are all equal. Although R_0 is only defined at the time of invasion, σ and R are defined at all times. We observe that $R \leq \sigma \leq R_0$ since after the infection has invaded a population and everyone is no longer susceptible, the replacement number R is always less than the basic reproduction number R_0. Also after the invasion, the susceptible fraction is less than one, so that not all adequate contacts result in a new case. Thus the replacement number R is always less than the contact number σ after the invasion.

Class	Meaning
S(t)	Susceptible inviduals
I(t)	Infective individuals
R(t)	Recovered individuals
E(t)	Exposed individuals
M(t)	Passively-immune infants

Table 2.1: Resume of classes names of compartmental models.

Symbol	Meaning
s(t)	Susceptible inviduals fraction
i(t)	Infective individuals fraction
r(t)	Recovered individuals fraction
e(t)	Exposed individuals fraction
m(t)	Passively-immune infants fraction
β	Contact rate
$\beta I(t)S(t)/N$	Standard incidence
$\beta I(t)S(t)$	Mass action incidence
δ	Passive immunity loss rate
$1/\delta$	Average period of passive immunity
ε	Latency loss rate
$1/\varepsilon$	Average latent period
γ	Recovery rate
$1/\gamma$	Average infectious period
μ	Birth / natural death rate
R_0	Basic reproduction number
σ	Contact number
R	Replacement number

Table 2.2: Resume of compartmental models notation.

2.3 Well-known compartmental models

In this section the most popular compartmental models are presented.

2.3.1 SIS model

In the SIS model two classes are taken into consideration: the susceptibles $S(t)$ and the infected $I(t)$. It is characterized by the fact recovery does not give immunity i.e. individuals move from the susceptible class to the infective class and then back to the susceptible one after they recover.

Figure (2.4) represents a basic endemic SIS model, that is a disease which is constantly present or very frequent in a population or territory. According to it vital dynamics of births and deaths are considered. In these terms other dynamics such as immigration/emigration could be taken into consideration, but in this section we do not for sake of simplicity. The model reads as following.

$$
\begin{cases}
\dfrac{dS(t)}{dt} = \mu N - \mu S(t) - \beta\, S(t)\, I(t)/N + \gamma I(t) \\[2mm]
\dfrac{dI(t)}{dt} = + \beta\, S(t)\, I(t)/N - \gamma I(t) - \mu I(t) \\[2mm]
(S(t_0),\, I(t_0)) = (S_0, I_0)
\end{cases}
\tag{2.6}
$$

$$
S(t) + I(t) = N
$$

where S_0 and I_0 are non-negative values which represent the initial number of susceptible or infected individuals at initial time t_0.
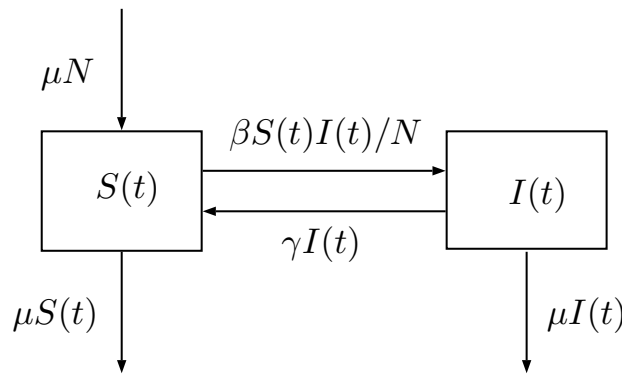
Figure 2.1: Flowchart of SIS endemic model (2.6).

Dividing the system (2.6) for the total population size N, and exploiting conservation law for N, which leads to $S(t) = N - I(t)$, the model is reduced to a one-variable system. It reads as

$$
\begin{cases}
\dfrac{di(t)}{dt} = + \beta\, i(t)\, (1 - i(t)) - (\gamma + \mu)\, i(t) \\[2mm]
i(t_0) = i_0
\end{cases}
\tag{2.7}
$$

where $0 < i_0 < 1$ represents theinfected fractions at initial time t_0 and $s(t) = 1 - i(t)$.
The solution of the initial value problem (2.7) is

$$
i(t) = \begin{cases}
\dfrac{e^{(\gamma+\mu)(\sigma-1)t}}{\sigma[e^{(\gamma+\mu)(\sigma-1)t} - 1]/(\sigma-1) + 1/i_0} & \text{for} \quad \sigma \neq 1, \\[4mm]
\dfrac{1}{\beta t + 1/i_0} & \text{for} \quad \sigma = 1,
\end{cases}
\tag{2.8}
$$

where σ is equal to the basic reproduction number R_0, which is defined as:

$$
R_0 = \sigma = \frac{\beta}{\gamma + \mu}
\tag{2.9}
$$

According to its meaning and the solution (2.8), it is easy to understand the following
equilibrium theorem.

Theorem 2.3.1 (Equilibrium of SIS model)**.**
Let $i(t)$ be the solution of (2.6) in $T = [0; 1]$. Then

- *If $R_0 = \sigma \leq 1$ then $i(t) \to 0$ as $t \to \infty$*

- *If $R_0 = \sigma \geq 1$ then $i(t) \to 1 - \frac{1}{\sigma}$ as $t \to \infty$*

The theorem (2.3.1) states that if the basic reproduction number R_0 is lower than
1, then the infections will decrease so that the disease will go to extinction. From a
mathematical point of view the model (2.6) has an unique disease free equilibrium
$E_0 = (S_0, 0)$ in the S-I plane and it is globally asymptotically stable.
Instead, if R_0 is greater than 1, the infection increases and the disease can not
be eliminated and it becomes endemic. In this case E_0 becomes unstable and an
endemic stable positive equilibrium $E^* = (S^*, I^*) = \left(\dfrac{1}{\sigma}N, \ N - \dfrac{1}{\sigma}N \right)$ appears.
Thus, $R_0 = 1$ represents the threshold whether the disease goes to extinction or goes
to an endemic.

2.3.2 SIR models

The SIR model is characterized by the fact that disease gives permanent immunity,
i.e. once an infected individual recovers he enters the recovered compartment $R(t)$,
which contains all individuals that cannot contract the infection again.

SIR epidemic model

The epidemic model (2.10) is used to describe outbreaks occurring in a short time period. Because of this reason vital dynamics (births, deaths, immigration, emigration, ...) are neglected and the model reads as

$$
\begin{cases}
\dfrac{dS(t)}{dt} = -\beta\, S(t)\, I(t)\, /N \\[2mm]
\dfrac{dI(t)}{dt} = \beta\, S(t)\, I(t)/N - \gamma I(t) \\[2mm]
\dfrac{dR(t)}{dt} = \gamma I(t) \\[2mm]
(S(t_0),\, I(t_0),\, R(t_0)) = (S_0,\, I_0,\, R_0)
\end{cases}
\tag{2.10}
$$

$$
S(t) + I(t) + R(t) = N
$$

where $S_0 > 0$, $I_0 > 0$, and $R_0 \geq 0$.
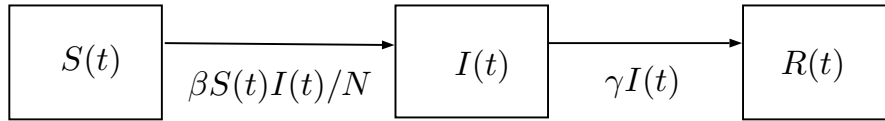
Figure 2.2: Flowchart of SIR epidemic model (2.10).

Here the contact number is

$$
\sigma = \frac{\beta}{\gamma}
\tag{2.11}
$$

corresponds to the product between the contact rate β per unit time and the average infectious period $1/\gamma$, i.e. it is the average number of adequate contacts of a typical infective individual during the infectious period.

The replacement number at initial time t_0, i.e. the basic reproduction number is the product of the contact number and the initial susceptible fraction

$$
R_0 = \sigma\, \frac{S_0}{N} = \frac{\beta}{\gamma N}\, S_0.
\tag{2.12}
$$

As for the SIS model (2.6), we can divide the model (2.10) by the constant total population size N and exploit the conservation law in the form $R(t) = N - S(t) - I(t)$

to reduce (2.10) into a two-variable system, which reads

$$\begin{cases} \dfrac{ds(t)}{dt} = -\beta\, s(t)\, i(t) \\[2ex] \dfrac{di(t)}{dt} = \beta\, s(t)\, i(t) - \gamma i(t) \\[2ex] (s(t_0),\, i(t_0)) = (s_0,\, i_0) \end{cases} \tag{2.13}$$

where $0 < s_0 < 1$, $0 < i_0 < 1$, and $r(t) = 1 - (s(t) + i(t))$.

According to the value of the basic reproduction parameter R_0 the following theorem describes the evolution of the disease.

Theorem 2.3.2 (Equilibrium of SIR epidemic model)**.**

Let $(s(t), i(t))$ be a solution of (2.13) in $T = \{(s, i) \mid s \geq 0,\ i \geq 0,\ s + i \leq 1\}$.

- *If $R_0 = \sigma \leq 1$, then $i(t)$ decreases to 0 as $t \to \infty$*

- *If $R_0 = \sigma > 1$, then $i(t)$ firstly increases up to a maximum value*

$$i_{max} = i_0 + s_0 - (1 + \ln(\sigma s_0))/\sigma$$

 and then decreases to 0 as $t \to \infty$. The susceptible fraction $s(t)$ is a decreasing function which tends to a limiting value s_∞.

Theorem (2.3.2) explains that the susceptibles $S(t)$ always decrease, but the final susceptible size S_∞ is positive.

If the basic reproduction number is lower than 1 then there is no epidemic and the disease tends to extinction i.e. $I(t) \to 0$ as $t \to \infty$.

Instead, if R_0 is greater than 1, $S(t)$ is still a decreasing function with positive limit S_∞ as $t \to \infty$, while the infective curve $I(t)$ firstly increases up to a maximum value $I_{max} = i_{max}N$ so that an epidemic occurs and then decreases to zero as $t \to 0$. The epidemic dies out because, when the susceptible size $S(t)$ goes below N/σ, the replacement number $\sigma S(t)/N$ goes below 1. It means that a typical infective individual initially replaces himself/herself with no more than one new infective so that infectives decrease and there is no epidemic. Figure (2.3) is an example of this last case, which represents the time evolution of the susceptible and infective fraction $s(t)$ and $i(t)$ with $R_0 > 1$.
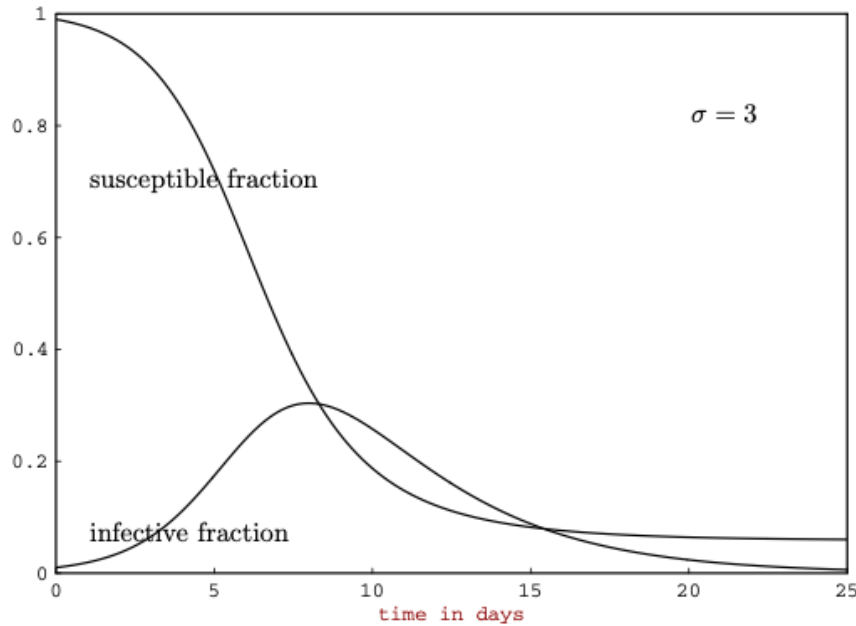
Figure 2.3: An example of solutions of the epidemic SIR model with contact number $\sigma = 3$ and average infectious period $1/\gamma = 3$ days.

SIR endemic model

The endemic model when takes into consideration birth and deaths reads as

$$
\begin{cases}
\dfrac{dS(t)}{dt} = \mu N - \mu S(t) - \beta\, S(t)\, I(t)/N \\[2mm]
\dfrac{dI(t)}{dt} = +\beta\, S(t)\, I(t)/N - \gamma I(t) - \mu I(t) \\[2mm]
\dfrac{dR(t)}{dt} = +\gamma I(t) - \mu R(t) \\[2mm]
(S(t_0),\, I(t_0),\, R(t_0)) = (S_0,\, I_0,\, \tilde{R}_0)
\end{cases}
\tag{2.14}
$$

$$ S(t) + I(t) + R(t) = N $$

where $S_0 > 0$, $I_0 > 0$, $\tilde{R}_0 > 0$.

The endemic SIR model is almost the same as the SIR epidemic model (2.10) described above, except that it has an inflow of newborns into the susceptible class at rate μN and deaths rates μS, μI, and μR in the relative classes. In this way deaths balance births, so that the population size N is constant.
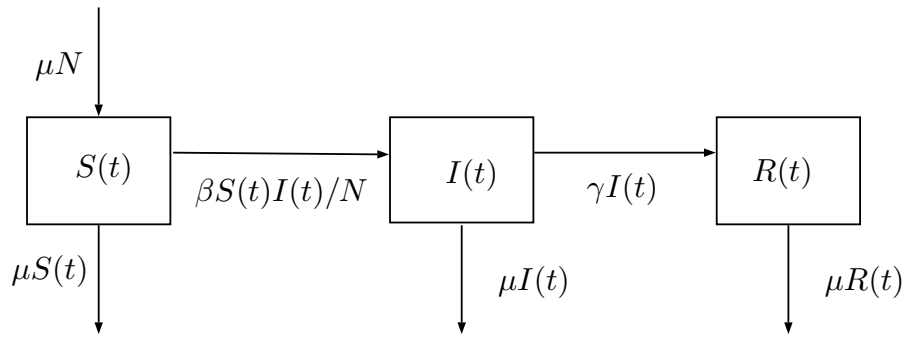
Figure 2.4: Flowchart of SIR endemic model (2.14).

In order to obtain the fractional version of the endemic SIR model (2.14) we divide equations (2.14) by the constant total population size N, exploit the conservation law of N, and obtain

$$
\begin{cases}
\dfrac{ds(t)}{dt} = \mu - \mu s(t) - \beta\, s(t)\, i(t) \\[2mm]
\dfrac{di(t)}{dt} = + \beta\, s(t)\, i(t) - \gamma i(t) - \mu i(t) \\[2mm]
(s(t_0),\, i(t_0)) = (s_0,\, i_0)
\end{cases}
\tag{2.15}
$$

where $0 < s_0 < 1$, $0 < i_0 < 1$ and $r(t) = 1 - s(t) - i(t)$.

For this model the threshold quantity is given by

$$
R_0 = \sigma = \frac{\beta}{\gamma + \mu}
\tag{2.16}
$$

and corresponds to the contact rate β multiplied by the average death-adjusted infectious period $1/(\gamma + \mu)$.

Theorem 2.3.3 (Equilibrium of SIR endemic model)**.**

Let $(s(t), i(t))$ be a solution of (2.18) in $T = \{(s, i) \mid s \geq 0,\ i \geq 0,\ s + i \leq 1\}$.

- *If $R_0 = \sigma \leq 1$, then solution paths starting in T approach the disease-free equilibrium given by $(s, i) = (1, 0)$.*

- *If $R_0 = \sigma > 1$, then all solution paths with $i_0 > 0$ approach the endemic equilibrium given by $E^* = (s^*, i^*) = \left(\dfrac{1}{\sigma},\ \mu\, \dfrac{\sigma - 1}{\beta} \right)$.*
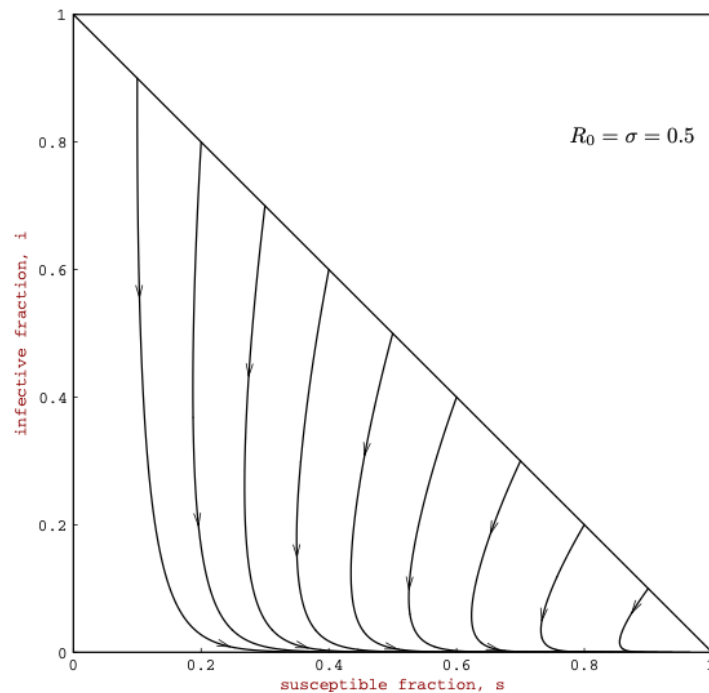
Figure 2.5: Phase plane (s,i) portrait for the classic SIR endemic model with contact number $\sigma = 0.5$.

Figures (2.5) and (2.6) illustrate the two possibilities given in the theorem. If the reproduction number R_0 is lower than 1, then the replacement number $R = \sigma s$ is less than 1 when $i_0 > 0$, so that the infectives decrease to zero. The infective fraction decreases rapidly to very near zero, and then after a large enough amount of years, the recovered people slowly die off and the birth process slowly increases the susceptibles, until eventually everyone is susceptible at the disease-free equilibrium with $(s,i) = (1,0)$. If R_0 is greater than 1 instead, then $R = \sigma s_0 > 1$ and $s(t)$ decreases while $i(t)$ increases up to a peak and then decreases, just as it would for an epidemic (compare Figure (2.6) to Figure (2.5)). However, after the infective fraction has decreased to a low level, the slow processes of deaths of recovered people and births of new susceptibles gradually increase the susceptible fraction until the replacement number $\sigma s(t)$ is large enough that another smaller epidemic occurs. This process of alternating rapid epidemics and slow regeneration of susceptibles continues as the paths approach the endemic equilibrium given in the theorem. This behaviour causes some oscillations of the system that are represented in Figure
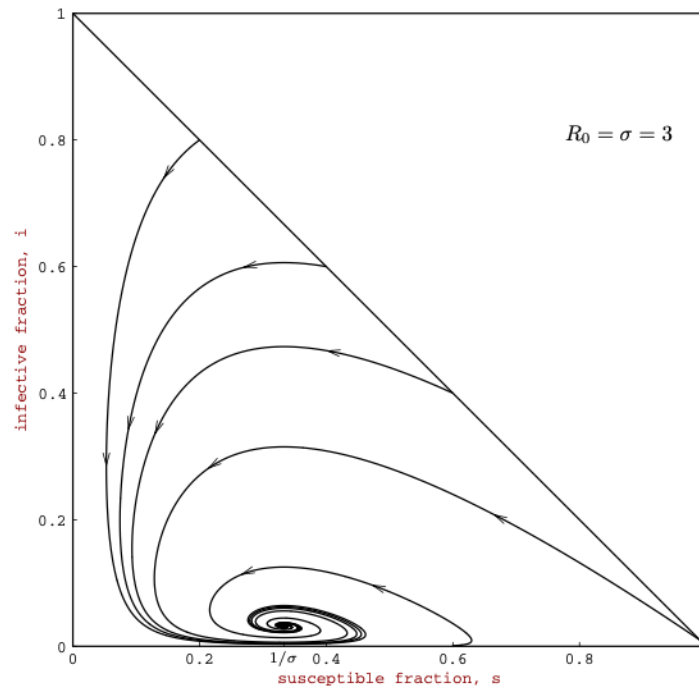
Figure 2.6: Phase plane (s, i) portrait for the classic SIR endemic model with contact number $\sigma = 3$, average infectious period $1/\gamma = 3$ days, and average lifetime $1/\mu = 60$ days. This unrealistically short average lifetime has been chosen so that the endemic equilibrium is clearly above the horizontal axis and the spiralling into the endemic equilibrium can be seen.

(2.6). At this endemic equilibrium the replacement number $R = \sigma s^*$ is 1, which is plausible since if the replacement number were greater than or less than 1, the infective fraction $i(t)$ would be increasing or decreasing, respectively.

For this SIR model there is a transcritical (stability exchange) bifurcation at $\sigma = 1$, as shown in Figure (2.7).

This equilibrium given by $(s^*, i^*) = (1/\sigma, \mu(\sigma - 1)/\beta)$ is unstable for $\sigma < 1$ and is locally asymptotically stable for $\sigma > 1$, while the disease-free equilibrium given by $(s, i) = (1, 0)$ is locally stable but unfeasible for $\sigma < 1$ and unstable for $\sigma > 1$. Thus these two equilibria exchange stabilities when $\sigma = 1$ and becomes a distinct, epidemiologically feasible, locally asymptotically stable equilibrium when $\sigma > 1$. This is called transcritical bifurcation and it corresponds to the exchange of stability of the two fixed points.

If the basic reproduction number R_0 (which is equal to the replacement number R when the entire population is susceptible) is less than 1, then the disease-free equilibrium is locally asymptotically stable and the disease cannot "invade" the population. But if $R_0 > 1$, then the disease-free equilibrium is unstable with a repulsive direction into the positive (s, i) quadrant, so the disease can spread in the sense that any path starting with a small positive i_0 moves into the positive (s, i) quadrant where the disease persists. Thus for this classic SIR endemic model the behavior is almost completely dependent on the threshold quantity R_0, which determines not only when the local stability of the disease-free equilibrium switches, but also when the endemic equilibrium enters the feasible region with a positive infective fraction.
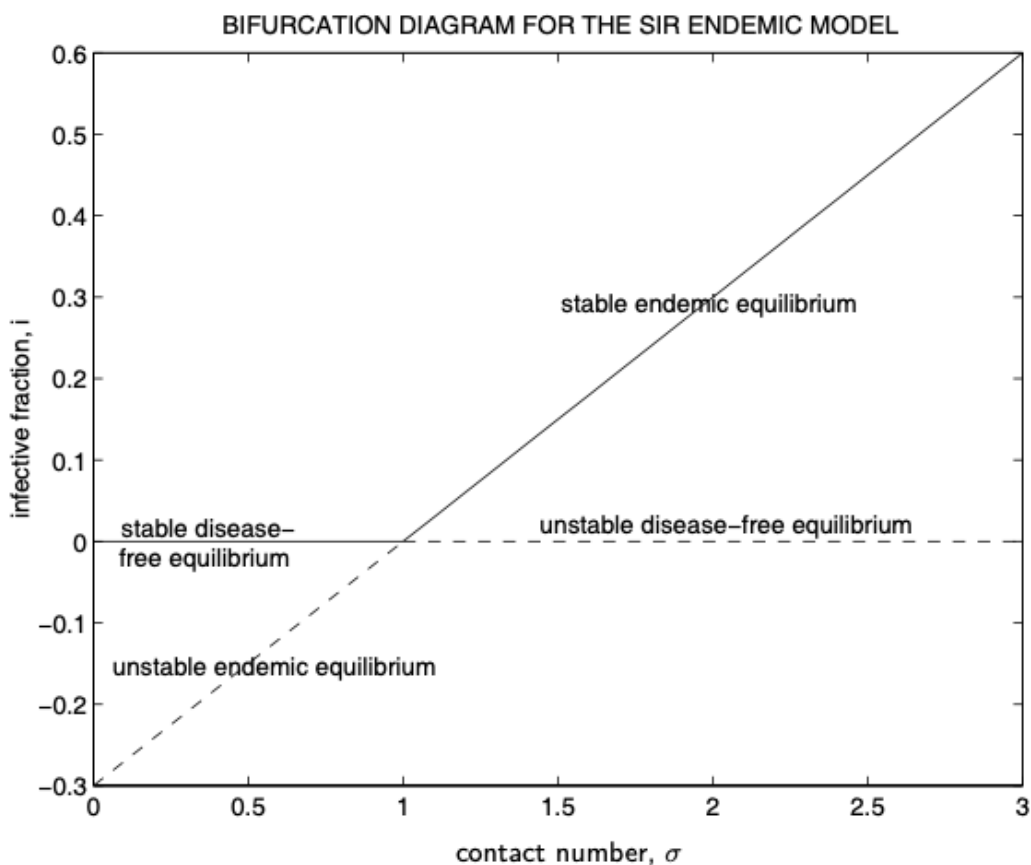
Figure 2.7: The bifurcation diagram for the SIR endemic model

2.3.3   SEIR epidemic model

We consider now the SEIR epidemic model, which has analogous behavior to that of the basic SIR epidemic model. This type of model assumes that when there is an adequate contact of a susceptible with an infective so that transmission occurs, then the susceptible enters the exposed class $E(t)$ of those in the latent period, who are infected, but not yet infectious. The incubation period is defined as the period from initial exposure to the appearance of symptoms. Since a person may becomes infectious before or after symptoms appear, the incubation period is often different from the latent period. In infectious disease modeling, we are always interested in the latent period, since we focus on the period until the person becomes infectious. After the latent period ends, the individual enters the class $I(t)$ of infectives, who are infectious in the sense that they are capable of transmitting the disease.

Since an epidemic occurs in a short time period, we ignore loss of temporary immunity and the birth/death and immigration/emigration processes. Further we have no flow from the removed class back to the susceptible class.

This model uses the standard incidence as mechanism of infection, and a transition from the exposed (latent) class $E(t)$ to the infected one $I(t)$ at rate $\varepsilon E(t)$, which corresponds to an exponential waiting time $e^{-\varepsilon t}$ with average latent period $1/\varepsilon$.

The model reads as

$$
\begin{cases}
\dfrac{dS(t)}{dt} = -\beta\, S(t)\, I(t)\,/N \\[2mm]
\dfrac{dE(t)}{dt} = \beta\, S(t)\, I(t)\,/N - \varepsilon\, E(t) \\[2mm]
\dfrac{dI(t)}{dt} = \varepsilon\, E(t) - \gamma I(t) \\[2mm]
\dfrac{dR(t)}{dt} = \gamma I(t) \\[2mm]
(S(t_0),\, R(t_0),\, I(t_0),\, R(t_0)) = (S_0,\, E_0,\, I_0,\, \tilde{R}_0)
\end{cases}
\tag{2.17}
$$

$$
S(t) + E(t) + I(t) + R(t) = N
$$

where $S_0 > 0$, $E_0 \geq 0$, $I_0 > 0$, and $\tilde{R}_0 \geq 0$.
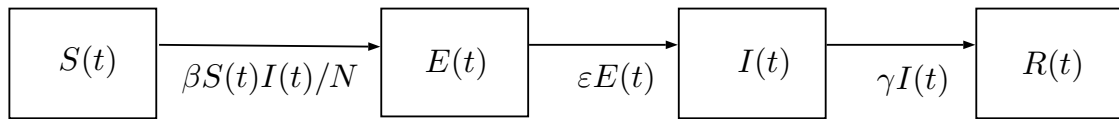
Figure 2.8: Flowchart of SEIR model (2.17).

Dividing the equations of the model (2.17) by the constant total population size N and exploiting the conservation of population size yield

$$\begin{cases} \dfrac{ds(t)}{dt} = -\beta\, s(t)\, i(t) \\[2mm] \dfrac{de(t)}{dt} = \beta\, s(t)\, i(t) - \varepsilon\, e(t) \\[2mm] \dfrac{di(t)}{dt} = \varepsilon\, e(t) - \gamma i(t) \\[2mm] (s(t_0),\, e(t_0),\, i(t_0)) = (s_0,\, e_0,\, i_0) \end{cases} \qquad (2.18)$$

where $0 < s_0 < 1$, $0 \geq e_0 < 1$, $0 < i_0 < 1$, and $r(t) = 1 - s(t) - e(t) - i(t)$. The tetrahedron T in the (s, e, i) phase plane given by

$$T = \{(s, e, i) \mid s \geq 0,\ e \geq 0,\ i \geq 0,\ s + e + i \leq 1\} \qquad (2.19)$$

is positively invariant and unique solutions exist in T for all positive time, so that the model is mathematically and epidemiologically well posed. As in the basic SIR epidemic model, the contact number $\sigma = \beta/\gamma$ corresponds to the contact rate β per unit time multiplied by the average infectious period $1/\gamma$, so it has the proper interpretation as the average number of adequate contacts of a typical infective during the infectious period. Moreover, the replacement number at time t_0 is still

$$R_0 = \sigma s_0. \qquad (2.20)$$

Theorem 2.3.4 (Equilibrium of SEIR model)**.**

Let $(s(t),\, e(t),\, i(t))$ be a solution of problem (2.17) in T defined in (2.24).

- *If $R_0 \leq 1$ then $e(t)$ and $i(t)$ decrease to zero as $t \to \infty$.*

- *If $R_0 > 1$, then $e(t) + i(t)$ first increases up a maximum with value*

$$e_{max} + i_{max} = e_0 + i_0 + s_0 - \frac{1}{\sigma} \ln(\sigma R_0) \tag{2.21}$$

and then decreases to zero as $t \to \infty$. The susceptible fraction $s(t)$ is a decreasing function and the limiting value s_∞ is the unique root in the interval $(0, \frac{1}{\sigma})$ of the equation

$$e_0 + i_0 + s_0 - s_\infty + \frac{1}{\sigma} \ln\left(\frac{s_\infty}{s_0}\right) = 0$$

.

The theorem asserts that, if the basic reproduction number R_0 is greater than 1, the SEIR model still has the typical epidemic outbreak as for the SIR epidemic model. The infective curve $i(t)$ first increases from an initial value i_0 near zero, reaches a peak of value (2.21), and then decreases towards zero as a function of time. As before, the susceptible fraction $s(t)$ always decreases, but the final susceptible fraction s_∞ is positive. The epidemic dies out because, when the susceptible fraction $s(t)$ goes below $1/\sigma$, the replacement number $\sigma s(t)$ goes below one. As before, if enough people are already immune so that a typical infective initially replaces itself with no more than one new infective, i.e. $\sigma s_0 \leq 1$, then there is no epidemic outbreak. But if a typical infective initially replaces itself with more than one new infective, i.e. $\sigma s_0 > 1$, then the infected curve initially increases so that an epidemic occurs. The speed at which an epidemic of a particular disease progresses depends on the contact rate β, the average latent period $1/\varepsilon$, and the average infectious period $1/\gamma$.

2.3.4   MSEIRS endemic model

The MSEIRS model proposed in this section takes into consideration latency and temporary immunity of disease. As in the SIR endemic model, let the birth and death rate constants be μ, so the population size N remains constant. The are two births contribution: the first one $\mu S(t)$ into the susceptible class of size $S(t)$ corresponds to newborns whose mothers are susceptible, and the other one $\mu(N - S(t))$ into the passively immune class of size $M(t)$, produced by mothers who were infected or had some type of immunity. Although all women would be out of the

passively immune class long before their childbearing years, theoretically a passively immune mother would transfer antibodies to her newborn child, so the infant would have passive immunity. Deaths occur in the epidemiological classes at the rates $\mu M(t)$, $\mu S(t)$, $\mu E(t)$, $\mu I(t)$, and $\mu R(t)$, respectively.

We introduce the *immunity loss constant* ρ that describe the progressive loss of immunity of the recovered individuals, so that there is a transition of $\rho R(t)$ individuals in the susceptible class.

Summing up, in this MSEIRS epidemiological model, the contagion mechanism is standard incidence, the transfer out of the passively immune class is $\delta M(t)$, the transfer out of the exposed class is $\varepsilon E(t)$, the recovery rate from the infectious class is $\gamma I(t)$, and the rate of loss of immunity is $\rho R(t)$. We remark that the linear transfer terms in the differential equations correspond to waiting times with negative exponential distributions, so that the mean passively immune period is $1/\delta$, the mean latent period is $1/\varepsilon$, the mean infectious period is $1/\gamma$, and the mean period of infection-induced immunity is $1/\rho$ [13]. The system of differential equations that describes the evolution of the epidemic is

$$
\begin{cases}
\dfrac{dM(t)}{dt} = \mu\,(N - S(t)) - (\,\delta + \mu\,)\,M(t) \\[2mm]
\dfrac{dS(t)}{dt} = \mu\,S(t) + \delta\,M(t) - \beta\,S(t)\,I(t)\,/N - \mu\,S(t) + \rho\,R(t) \\[2mm]
\dfrac{dE(t)}{dt} = \beta\,S(t)\,I(t)\,/N - (\,\varepsilon + \mu\,)\,E(t) \\[2mm]
\dfrac{dI(t)}{dt} = \varepsilon\,E(t) - (\,\gamma + \mu\,)\,I(t) \\[2mm]
\dfrac{dR(t)}{dt} = \gamma\,I(t) - (\,\rho + \mu\,)\,R(t) \\[2mm]
(\,M(t_0),S(t_0),R(t_0),I(t_0),R(t_0)) = (M_0,\,S_0,\,E_0,\,I_0,\,\tilde{R}_0)
\end{cases}
\tag{2.22}
$$

$$
M(t) + S(t) + E(t) + I(t) + R(t) = N
$$

where $M_0 > 0$, $S_0 > 0$, $E_0 \geq 0$, $I_0 > 0$, and $\tilde{R}_0 > 0$.
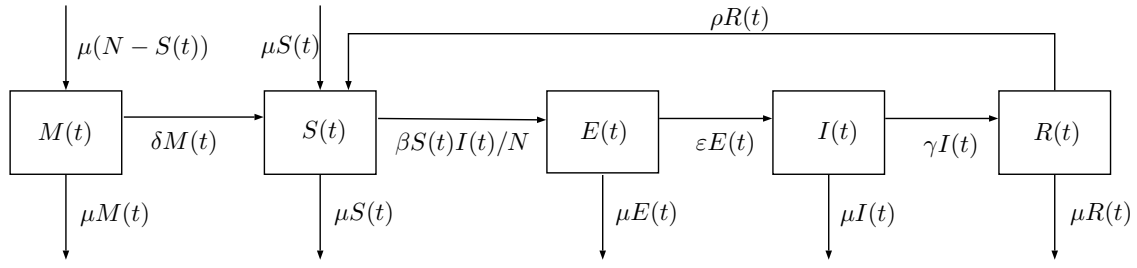
Figure 2.9: Flowchart of MSEIRS model (2.22).

For sake of simplicity to neglect time dependencies and to convert the system (2.22) to the normalized epidemiological model through dividing by the constant population size N and eliminating the differential equation for $s(t)$ exploiting the conservation law for total population size. Then the ordinary differential system for the MSEIRS model is

$$
\begin{cases}
\dfrac{dm}{dt} = \mu\,(e+i+r) - \delta\,m \\[2mm]
\dfrac{de}{dt} = \beta\,i\,(1-m-e-i-r) - (\varepsilon + \mu\,)\,e \\[2mm]
\dfrac{di}{dt} = \varepsilon\,e - (\gamma + \mu\,)\,i \\[2mm]
\dfrac{dr}{dt} = \gamma I(t) - (\rho + \mu\,)\,r \\[2mm]
(m(t_0),\, e(t_0),\, i(t_0),\, r(t_0)) = (m_0,\, e_0,\, i_0,\, r_0)
\end{cases}
\tag{2.23}
$$

where $0 < m_0 < 1$, $0 \geq e_0 < 1$, $0 < i_0 < 1$, $0 < r_0 < 1$, and $s = 1 - m - e - i - r$
A suitable domain is

$$
D = \{\,(m,s,e,i)\,|\,m \geq 0,\; s \geq 0,\; e \geq 0,\; i \geq 0,\; m+s+e+i \leq 1\}
\tag{2.24}
$$

which is positively invariant, because no solution paths leave through any boundary. Since paths cannot leave D, solutions exist for all positive time. Thus the model is mathematically and epidemiologically well posed.

   The basic reproduction number R_0 for this MSEIRS model is equal to the the contact number σ and it is given by the product of the contact rate β per unit time,

the average infectious period adjusted for population growth of $1/(\gamma+\mu)$, and the fraction $\varepsilon/(\varepsilon+\mu)$ of exposed people surviving the latent class $E(t)$ i.e.

$$R_0 = \sigma = \frac{\beta\varepsilon}{(\gamma+\mu)(\varepsilon+\mu)} \tag{2.25}$$

R_0 has the correct interpretation as the average number of secondary infections due to an infective during the infectious period, when everyone in the population is susceptible.

The equations (2.23) always have a disease-free equilibrium given by $m=e=i=r=0$ and $s=1$. If $R_0 > 1$, there is also a unique endemic equilibrium in D given by

$$
\begin{cases}
m^* = \dfrac{\mu}{\delta+\mu}\left(1-\dfrac{1}{R_0}\right) \\[2ex]
e^* = \dfrac{\delta(\gamma+\mu)(\rho+\mu)}{(\delta+\mu)[(\rho+\mu)(\gamma+\varepsilon+\mu)+\gamma\varepsilon]} \\[2ex]
i^* = \dfrac{\delta\varepsilon(\rho+\mu)}{(\delta+\mu)[(\rho+\mu)(\gamma+\varepsilon+\mu)+\gamma\varepsilon]} \\[2ex]
r^* = \dfrac{\delta\varepsilon\gamma}{(\delta+\mu)[(\rho+\mu)(\gamma+\varepsilon+\mu)+\gamma\varepsilon]}
\end{cases}
\tag{2.26}
$$

where $s^* = \dfrac{1}{R_0} = \dfrac{1}{\sigma}$.

Note that the replacement number is 1 at the endemic equilibrium i.e. $R^* = \sigma s^* = 1$. By linearization, the disease-free equilibrium is locally asymptotically stable if $R_0 < 1$, while when $R_0 > 1$ it is unstable with a stable manifold outside D and an unstable manifold into D. The disease-free equilibrium can be shown to be globally asymptotically stable in D if $R_0 \leq 1$ by using the Liapunov function

$$V = \varepsilon e(t) + (\varepsilon + \mu)i(t). \tag{2.27}$$

Since $\beta\varepsilon \leq (\varepsilon + \mu)(\gamma + \mu)$ the Liapunov derivative is negative:

$$\dot{V} = [\beta\varepsilon s(t) - (\varepsilon + \mu)(\gamma + \mu)]i(t) \leq 0. \tag{2.28}$$

The set where $\dot{V} = 0$ is the face of D with $i(t) = 0$, but $\dfrac{di(t)}{dt} = \varepsilon e(t)$ on this face, so that $i(t)$ moves off the face unless $e(t) = 0$. Further, when $e(t) = i(t) = 0$ then

$\frac{dr(t)}{dt} = -\mu\, r(t)$, so that $r(t) \to 0$ as $t \to \infty$, and $e(t) = i(t) = r(t) = 0$, then $\frac{dm(t)}{dt} = -\delta m(t)$, so $m \to 0$ as $t \to 0$. Because the origin is the only positively invariant subset of the set with $\dot{V} = 0$, all paths in D approach the origin by the Liapunov–Lasalle theorem (see Appendix A). Thus if $R_0 \leq 1$, then the disease-free equilibrium is globally asymptotically stable in D. The characteristic equation corresponding to the Jacobian at the endemic equilibrium is a fourth degree polynomial. It has been shown [18] that the Routh–Hurwitz criteria (see Appendix B) are satisfied if $R_0 > 1$, so that the endemic equilibrium (2.26) is locally asymptotically stable when it is in D. Thus if $R_0 > 1$, then the disease-free equilibrium is unstable and the endemic equilibrium is locally asymptotically stable.

2.4 Refined model

According to the increasing interest in mathematical epidemiology, different and more accurate models have been proposed. Along with them new population classes have been introduced.

In this section we will deal with the dynamics that regards quarantine and vaccination, since these are surely relevant factors aiming at controlling the epidemic. The two models taken into consideration are the so called SIQS and SIS-VS model.

We need to introduce two new classes that are:

- The **quarantined compartment** $Q(t)$, in which all individuals whom, once they discover they are infected, isolate themselves from other people, so that they cannot have any contact with other individuals.

- The **vaccinated compartment** $V(t)$, in which all individuals are vaccinated therefore immune to the virus.

In the following model we leave the hypothesis of conservation of total population size.

2.4.1   SIQS & SIQR - Quarantine models

Although isolation is probably always a desirable public health measure, quarantine is more controversial. Mass quarantine can inflict significant social, psychological, and economic costs without resulting in the detection of many infected individuals as we can testify during this period. When isolation is ineffective, the use of quarantine becomes beneficial when there is significant asymptomatic transmission. The earliest study on the effects of quarantine on the transmission of the infection is achieved by Feng and Thieme [15] and Wu and Feng [16].

The SIQS and SIQR models proposed in this section include the following classes: susceptibles $S(t)$, infected $I(t)$, quarantined $Q(t)$ and, only for the SIQR model, the recovered $Q(t)$. We remember that the recovered class is not present in the SIS model because in this case disease does not entails immunity.

The following hypothesis are assumed.

1. Two deaths rates are taken into consideration:

   - $\tilde{d} \geq 0$, the natural deaths rate;

   - $\alpha \geq 0$, the disease deaths rate, which represents the deaths caused by the disease, that effects infected and quarantined individuals.

2. $A \geq 0$ is the number of newborns per unit time that enters the class of susceptibles.

3. Only a fraction $0 \leq \delta \leq 1$ of infected individuals gets into quarantine: if $\delta = 1$ all infected individuals quarantine, while if $\delta = 0$ none of them does.

4. $0 \leq \eta \leq 1$ is the fraction of individuals that finishes the quarantine: $1/\eta$ is the average period of quarantine, after which a quarantined individual recovers and returns to the susceptible class in SIQS model or enters the recovered in the SIQR model.

SIQS model

In this SIQS model the simple mass action incidence $\beta S(t) I(t)$ is used. Another possible form, apart from the standard incidence, could have been the quarantine adjusted incidence that is $\dfrac{\beta S(t) I(t)}{N - Q(t)}$. The SIQS model reads as

$$
\begin{cases}
\dfrac{dS(t)}{dt} = A - \beta I(t) S(t) - \tilde{d} S(t) + \gamma I(t) + \eta Q(t) \\[2mm]
\dfrac{dI(t)}{dt} = \beta S(t) I(t) - (\gamma + \delta + \tilde{d} + \alpha) I(t) \\[2mm]
\dfrac{dQ(t)}{dt} = \delta I(t) - (\eta + \tilde{d} + \alpha) Q(t) \\[2mm]
(S(t_0), I(t_0), Q(t_0)) = (S_0, I_0, Q_0)
\end{cases}
\tag{2.29}
$$

$$
S(t) + I(t) + Q(t) = N(t)
$$

where $S_0 > 0$, $I_0 > 0$, and $Q_0 \geq 0$.

Here the basic reproduction number is

$$
R_0 = \frac{\beta \dfrac{A}{\tilde{d}}}{(\gamma + \delta + \tilde{d} + \alpha)}
\tag{2.30}
$$

and is given by the product between the contact rate β, the average infectious period adjusted for population growth and quarantine $1/(\gamma + \delta + \tilde{d} + \alpha)$ and the number of newborn respect to deaths $A/\tilde{d}$.
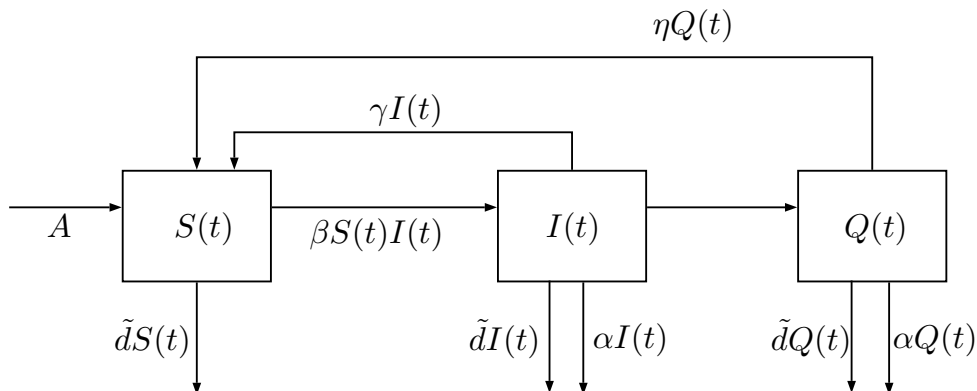

Figure 2.10: Flowchart of SIQS model (2.29).

Theorem 2.4.1 (Equilibrium of SIQS model).

Let the basic reproduction number be $R_0 = \dfrac{\beta A}{(\gamma + \delta + \tilde{d} + \alpha)\,\tilde{d}}$. *Then*

- *If* $R_0 \leq 1$ *then the disease free equilibrium* $E_0 = (S_0, 0, 0)$ *of the model* (2.29) *is globally asymptotically stable;*

- *If* $R_0 > 1$, E_0 *is unstable and there exists an endemic equilibrium* $E^* = (S^*, I^*, Q^*)$ *which is globally asymptotically stable*

It means that in the first case, when $R_0 \leq 1$, the epidemic expires and the number of infected individuals goes to 0, as the number of quarantined. If the basic reproduction number is greater than 1, then the disease-free equilibrium is not asymptotically stable anymore, and a new equilibrium which allows the coexistence of the three classes arises.

SIQR model

In this subsection the SIQR model is proposed. Here the quarantine adjusted incidence is used i.e. the transmission occurs as $\dfrac{\beta S(t) I(t)}{N - Q(t)} = \dfrac{\beta S(t) I(t)}{S(t) + I(t) + R(t)}$.
The SIQS model reads as

$$
\begin{cases}
\dfrac{dS(t)}{dt} = A - \dfrac{\beta I(t) S(t)}{S(t) + I(t) + R(t)} - \tilde{d} S(t) \\[3mm]
\dfrac{dI(t)}{dt} = \dfrac{\beta I(t) S(t)}{S(t) + I(t) + R(t)} - (\gamma + \delta + \tilde{d} + \alpha) I(t) \\[3mm]
\dfrac{dQ(t)}{dt} = \delta I(t) - (\eta + \tilde{d} + \alpha) Q(t) \\[3mm]
\dfrac{dR(t)}{dt} = \gamma I(t) + \eta Q(t) - \tilde{d} R(t) \\[3mm]
(S(t_0),\, I(t_0),\, Q(t_0),\, R(t_0)) = (S_0,\, I_0,\, Q_0,\, \tilde{R}_0)
\end{cases}
\tag{2.31}
$$

$$
S(t) + I(t) + Q(t) + R(t) = N(t)
$$

where $S_0 > 0$, $I_0 > 0$, $\tilde{R}_0 > 0$ and $Q_0 \geq 0$.
Here the basic reproduction number is

$$
R_0 = \frac{\beta}{(\gamma + \delta + \tilde{d} + \alpha)}
\tag{2.32}
$$

and is given by the product between the contact rate β and the average infectious period adjusted for population growth and quarantine $1/(\gamma + \delta + \tilde{d} + \alpha)$.
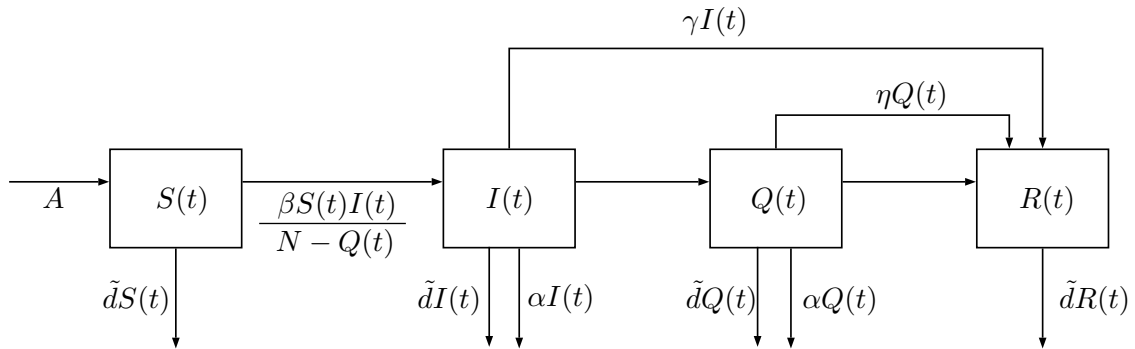
Figure 2.11: Flowchart of SIQR model (2.29).

Theorem 2.4.2 (Equilibrium of SIQR model)**.**

Let the basic reproduction number be $R_0 = \dfrac{\beta}{(\gamma + \delta + \tilde{d} + \alpha)}$. *Then*

- *If* $R_0 \leq 1$ *then the disease free equilibrium* $E_0 = \left(\dfrac{A}{\tilde{d}}, 0, 0, 0\right)$ *of the model (2.29) is locally stable;*

- *If* $R_0 > 1$, *the disease free equilibrium* E_0 *is unstable and there exists an endemic equilibrium* $E^* = (S^*, I^*, Q^*, R^*)$ *which is locally stable and Hopf bifurcation can occur for some parameter values, so that* E^* *is sometimes an unstable spiral and a periodic solution around* E^* *can occur.*

The theorem explains that a locally stable epidemic free equilibrium is there when the basic reproduction number is under the threshold $R_0 = 1$, while when it goes beyond it this equilibrium becomes unstable and an epidemic equilibrium appears, with the possibility of periodic orbit. Only in the SIQR model with the quarantine-adjusted incidence a periodic solution around the endemic equilibrium may exist, which is produced by Hopf bifurcation, for all the other models presented in this chapter, the endemic equilibrium is always globally asymptotically stable.

2.4.2 SIS-VS - vaccination model

The model that is proposed in this section represents one of the most powerful responses to the epidemic. This is the SIS-VS model, which includes the possibility to vaccinate the population. The vaccinated compartment $V(t)$ is introduced. In this class all individuals are vaccinated therefore immune to the virus.

The following hypothesis hold:

1. The birth is $r \in [0; 1]$ and the total number of newborns is $rN(t)$, while $d \in [0; 1]$ is the natural death rate.

2. An homogeneous portion among the susceptible population and the newborn is vaccinated: p and q are the proportional coefficients of vaccinated from susceptible and newborn respectively.

3. Immunity caused by the vaccination is temporary: $\eta > 0$ is the immunity loss rate and $1/\eta$ represents the average period over which the vaccination is effective after which the vaccinated individual turns back to the susceptible compartment.

4. Even if an individual has been vaccinated, he still has a certain probability to be infected; $\sigma \in [0; 1]$ is the fraction that reflects the reduction of efficiency of the vaccine, $\sigma = 0$ means that the vaccine is completely effective in preventing infection.

The disease spreads with the standard incidence function and, neglecting time dependencies in sake of simplicity, the model reads as

$$
\begin{cases}
\dfrac{dS}{dt} = r(1-q)N - \beta IS/N + \gamma I - (p+d)S + \eta V \\[2mm]
\dfrac{dI}{dt} = +\beta SI/N + \beta \sigma VI/N - (\gamma + \alpha + d)I \\[2mm]
\dfrac{dV}{dt} = qN + pS - (\eta + d)V - \beta \sigma VI/N \\[2mm]
(S(t_0),\, I(t_0),\, V(t_0)) = (S_0,\, I_0,\, V_0)
\end{cases}
\tag{2.33}
$$

$$S + I + V = N$$

According to this model the total population size evolves in time as

$$\frac{dN}{dt} = -N[r-d]\alpha I \tag{2.34}$$

where S_0, I_0, V_0 are non-negative initial values.
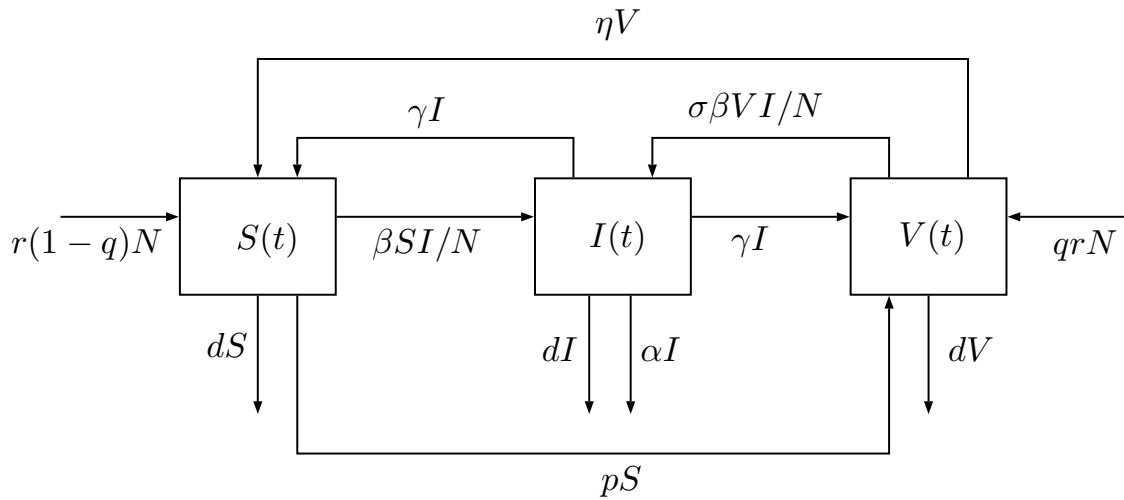
Figure 2.12: Flowchart of SIV-VS model (2.33).

Take the transformation $s = \dfrac{S}{N}$, $i = \dfrac{I}{N}$, and $v = \dfrac{V}{N}$, and assume that the deaths rate is equal to the births rates i.e. $d = r$, for sake of simplicity. The following model is obtained:

$$\begin{cases} \dfrac{di}{dt} = +\beta\, s\, i + \beta\sigma vi - (\gamma + \alpha + r)\, i \\[2mm] \dfrac{dv}{dt} = qN + p\, s - (\varepsilon + r)\, v - \beta\sigma vi \\[2mm] (\, i(t_0)\,,\, v(t_0)) = (i_0,\, v_0) \end{cases} \tag{2.35}$$

$$s = 1 - i - v$$

Theorem 2.4.3 (Equilibrium of SIV model)**.**

Let

$$R_0 = \frac{\beta\,[\varepsilon + \sigma p + r\,(1 - (1-\sigma)\,q)]}{(\alpha + r + \gamma)\,(p + \varepsilon + r)} \tag{2.36}$$

be the basic reproduction number of system (2.35) and let $D = \{ (s,i,v) \mid s \geq 0, i \geq 0, v \geq 0, s+i+v \leq 1 \} \subset \mathbb{R}^3$ be the domain of the problem. Then:

1. If $R_0 > 1$ then the endemic equilibrium E^* exists and is globally asymptotically stable;

2. If $R_0 \leq 1$, $\alpha < \sigma\beta$, $\beta > r+\gamma+\alpha$, and $B \geq 2\sqrt{AC}$ then there exist two endemic equilibria $E_1^* = (i_1^*, v_1^*)$ and $E_2^*(i_2^*, v_2^*)$, with $i_1^* < i_2^*$ and $v_1^* > v_2^*$ and two stable manifolds which divide the region $\hat{D} = \{ (i,v) \mid i \geq 0, v > 0, i+v < 1 \}$ into two parts D_1 and D_2 such that:

$$\lim_{t \to \infty} (i(t), v) = (0, v_0) \quad when \quad (i_0, v_0) \in D_1$$

$$\lim_{t \to \infty} (i(t), v(t)) = (i_2^*, v_2^*) \quad when \quad (i_0, v_0) \in D_2$$

where:

$A = (\alpha - \sigma\beta)(\beta - \alpha)$

$B = \alpha(p+\varepsilon+\gamma+\alpha+2r) - \beta\left[(\alpha+r+\varepsilon) - \sigma(\beta-r-\alpha+\gamma-p)\right]$

$C = \beta(p+r+\varepsilon) - \beta(1-\sigma)(rq+p) - (p+r+\varepsilon)(r+\alpha+\gamma)(R_0-1)$

3. If $R_0 = 1$, $\alpha < \sigma\beta$, $\beta > r+\gamma+\alpha$, $B = 2\sqrt{AC}$, then there exist an endemic equilibrium E_3^* and two stable manifolds of this equilibrium which divide the region D into two parts D_1 and D_2 such that:

$$\lim_{t \to \infty} (i(t), v(t)) = (0, v_0) \quad when \quad (i_0, v_0) \in D_1$$

$$\lim_{t \to \infty} (i(t), v(t)) = (i_2^*, v_2^*) \quad when \quad (i_0, v_0) \in D_2$$

4. If $R_0 < 1$, $\alpha < \sigma\beta$, $B > 0$ then there exist an endemic equilibrium E_3^* which is globally asymptotically stable.

5. If the parameters do not satisfy the cases (1-4) then the disease free equilibrium $E_0 = (0, z_0)$ is globally asymptotically stable.

This theorem shows the presence of a backward bifurcation based on the value of the basic reproduction number. When R_0 is lower than the critical value R_c, the disease extinguishes and the only infective-free equilibrium E_0 is possible. The critical value

R_c represents the threshold the number of equilibria changes, after which an endemic equilibrium arises, with two stable manifolds. When R_0 overcomes the value one, then the endemic equilibrium becomes globally asymptotically stable.

Chapter 3

SARS-CoV-2: the virus and the immune system reaction

3.0.1 The virus SARS-CoV-2

In December 2019, in the city of Wuhan, capital of Hubei Province, Chinese health authorities identified a cluster of pneumonia cases of unknown aetiology [23]. The investigations undertaken led to the identification of a new SARS-CoV-2 coronavirus, of the same family as those responsible for Severe Acute Respiratory Syndrome (SARS-CoV) and Middle Eastern Respiratory Syndrome (MERS-CoV). The new virus that causes the disease called Covid-19 (Corona-virus disease) has rapidly spread around the world and on 11 March 2020 the Emergency Committee of the World Health Organization (WHO) declared a pandemic. A pandemic is the spread of an epidemic disease in large geographical areas on a global scale, consequently involving a large part of the world population, either in the disease itself or in the risk of contracting it. This situation presupposes the lack of human immunization towards a highly dangerous pathogen.

Corona-viruses, first described in 1966 by Tyrell and Bynoe [24], are a family of single-stranded RNA viruses that infect humans, but also a wide range of animals. There are four subfamilies of corona-viruses: alpha and beta (apparently coming from mammals, especially bats), gamma and delta (coming from pigs and birds). Among the subtypes of corona-viruses that can infect humans, beta-coronaviruses,

to which SARS-CoV-2 belongs, can cause serious illness and death, while alpha corona-virus causes mildly symptomatic or asymptomatic infections [25], [26]. Although SARS-CoV-2 originated from bats [27], the intermediate animal through which it passed to humans is uncertain. Pangolins and snakes are the current suspects.

The main four genes of SARS-CoV-2 include four structural proteins: nucleocapsid protein (N), spike protein (S), envelope protein (E) and membrane protein (M) [28]. In the Receptor Binding Domain (RBD), the binding of the spike protein allows the virus to attack, fuse and enter the host cells. The viral RNA is then released into the cytoplasm, replicated and translated for the formation of new viral particles.

The spread

SARS-CoV-2 infection mainly affects the lower respiratory tract. Human-to-human airway transmission is undoubtedly the main source of contagion, which occurs mainly through relatively large droplets of mucus produced when a person carrying the virus sneezes or coughs. Other ways of transmission are aerosol or contaminated surfaces. In this last case, the virus contained in the droplets, deposited on the surfaces and remained active, is transmitted to another individual through contaminated hands that come into contact with the oral, nasal or conjunctival mucosa. Virus particles are present in the secretions of the respiratory system of an infected person and can contaminate others through direct contact with mucous membranes [29] with an average incubation period of between 2 and 12 days [30].

The presence of active virus in faeces has also been found in Covid-19 patients. These results demonstrate that, in addition to direct contact and contact with patients' respiratory secretions, the virus can also be transmitted by fecal-oral route [31]. This means faeces samples can contaminate hands, food, water, etc. and can cause infections by invading the oral cavity, respiratory mucosa, conjunctiva, etc.

According to current information, there are no cases of transplacental transmission from pregnant women to their fetus, while cases of neonatal disease due to postnatal transmission have been described [32].

The transmission from one individual to another of SARS-CoV-2 can happen in

many ways. This fact partially explain the strength and the speed of contagion.

3.0.2   Immune response to infection

The possibilities for the immune system to intervene to defend the body against the
virus are many and involve both the innate and adaptive immune responses, both
with their humoral and cellular components.

Innate immunity

SARS-CoV-2 is a new human coronavirus, therefore antigenically different from
other viruses and specifically from other human corona-viruses. This implies that
no human has ever been infected with this virus prior to its spread in November-
December 2019. Furthermore, the fact that SARS-CoV-2 is antigenically different
from other viruses means that no human being could have, before possible infection,
antibodies or cells of the immune system reactive against this virus, apart from
possible cross-reactivity with other similar viruses. Theoretically, in November-
December 2019, the whole of humanity could be considered susceptible to infection
with SARS-CoV-2. However, having specific antibodies to a given pathogen does
not mean that an individual is entirely devoid of any defense. The immune system,
in fact, is able to protect us not only thanks to antibodies or cells that selectively
recognize individual infectious agents, but also thanks to the intervention of a se-
ries of factors and cells which, by identifying certain microorganisms as potentially
harmful, try to limit their virulence in a non-selective manner. The set of these
factors and cells is called the "innate immune system", indicating that it is present
and functioning even before there are those infectious experiences that induce the
production of antibodies and specific cells for certain microorganisms. Antibodies
and specific cells are part of the "adaptive immune system" and, after an infectious
disease, they remain for a long time as an immunological memory of the infection ca-
pable of preventing subsequent contact with the same infectious agent from causing
the same disease again.

The innate immune system is certainly able to limit the aggressiveness of SARS-
CoV-2. Most people who become infected with this virus, in fact, have a mild disease,

sometimes unapparent or identified by fever and other flu-like symptoms limited to the upper airways. In these cases, regardless of possible cross-reactivity not yet demonstrated, it must be assumed that the infected person has been protected by the innate immune system through the various mechanisms that characterize it.

The innate immune system has various mechanisms of protection from infectious agents that are strategically placed in the anatomical sites where there is the greatest risk of contact with pathogens. In the case of Covid-19, the infection occurs mainly by inhalation of droplets, Flügge droplets or aerosols containing SARS-CoV-2 exhaled with coughing, sneezing or conversation with contagious subjects. The defense systems of the upper airways are therefore particularly important. The anatomy of the nose favors the contact of the inhaled air with the walls of the nasal and retropharyngeal mucosa, where the mucus retains particles and cells and the factors of the innate immune system can interact with the virus. One of the main virus protection mechanisms of the innate immune system is the production of interferons IFNs by infected cells. Viruses, in order to replicate and then infect other individuals, must enter the host cells and monopolize their protein synthesis system. Type I IFNs and cytokines are factors produced by infected cells that are capable of reducing viral replication in other cells by various mechanisms including the limitation of protein synthesis. Some among immune cells could identify infected cells by recognizing the variation induced by viral infection in membrane expression of some molecules and consequently kill the infected cell before the virus can replicate itself extensively.

However, the literature data do not agree in identifying these humoral or cellular factors of the innate immune system as the main elements responsible for protection from SARS-CoV-2. Unlike other corona-viruses, such as SARS-CoV and MERS, this virus does not seem to be capable of stimulating the release of high amounts of type I IFN [36], [37] and evidence of the role of innate immune cells is scarce [38]. Other potentially protective factors of the innate immune system in the mucous membranes that could contribute to the defense against SARS-CoV-2 are the natural immunoglobulins (Ig) of the IgM, IgA and IgG classes. Natural immunoglobulins are present at birth and are produced by a subpopulation of lymphocytes, probably as a result of non-selective stimulation by their own antigens. A classic example

is immunoglobulins capable of recognizing antigenic glycoproteins specific to blood
groups. The subjects of group *0* possess the natural antibodies Ig that are capable
of recognizing the red cells expressing glycoprotein antigens of groups *A* and *B*, even
in the absence of previous contacts with these red cells, while the subjects of group
AB do not have such antibodies. In the same way the natural Ig could prevent the
binding of the virus to its receptor on the host cell and consequently have a neu-
tralizing role. Particularly interesting is the observation that natural IgM decreases
significantly with age and after 55-60 years the levels are very low. This observation
could explain the increased susceptibility to more severe forms of Covid-19 in the
elderly.

The possible role of mannose-binding lectin (MBL) is also particularly interesting.
The concentration of this factor of the innate immune system also decreases signif-
icantly with age and its intervention could be particularly important in protecting
against SARS-CoV-2 infection [39]. Indeed, glycans rich in mannose on protein S
could bind MBL [40] and thereby inhibit the binding of the viral surface protein to
its receptor on the human cell.

The complement system is another factor of innate immunity that can promote in-
flammation and protect against SAR-CoV-2 infection. It can be activated by the
lectin, which is triggered by the MBL itself and acts by recruitment of inflamma-
tory cells and the release of cytokines at the infection sites. Specific studies will be
necessary to establish which, among the mechanisms mentioned or even others, are
actually operating in the innate defense against SARS-CoV-2.

Adaptive immunity and viral clearance

Respiratory epithelial cells infected with SARS-CoV-2 produce virus proteins from
viral RNA. These proteins are processed within the cell and the derived peptide
fragments are presented to CD8 + cytotoxic T lymphocytes [40]. Activated CD8 +
T lymphocytes multiply with development of "memory T lymphocytes" and virus-
specific cytotoxic effectors that are capable of lysing virus-infected tissue cells. At the
same time, for a brief period, the whole virus or its fragments are recognized by the
cells presenting the antigen. These cells are mainly dendritic cells and macrophages

that present CD4 + T cell viral peptides. B cells can directly recognize viruses and activate and / or interact with CD4 + T cells to produce antibodies. During SARS-CoV-2 infection with mild to moderate clinical course, an increase in B lymphocytes, follicular helper T lymphocytes, CD8 + and CD4 + T cells activated at the time of viral clearance was observed with further increase in the following days.

The primary antibody response, represented by the appearance of IgM virus antibodies, is usually observed within the first week after the onset of symptoms and before their disappearance [41]. The appearance of IgG antibodies follows and partly overlaps with the early IgM response. The antibodies mainly recognize protein epitopes S, N and to a lesser extent M. Some anti-virus IgG antibodies, called neutralizing antibodies, are functionally protective, i.e. able to block the entry of the virus into the cell, making the subject immune to viral infection.

Immune hyperactivation: cytokine storm

A large percentage of people infected with SARS-CoV-2 may experience more severe disease, involving the lower airways and pneumonia requiring appropriate care and support. In addition, a more limited number of subjects may experience respiratory complications and involvement of other organs and systems that create Covid-19 a very severe and fatal disease, especially in subjects of advanced age and with other concomitant diseases (comorbidities). A particularly high level of serum cytokines was observed in these subjects [42], [43], [44]. This finding is in some ways in contrast to the observation that SARS-CoV-2, unlike SARS-CoV, is less capable of stimulating the secretion of inflammatory cytokines in lung cells [45]. On the other hand, it has been observed that the aggravation of the disease and the detection of high dosages of cytokines in the serum of patients with more severe disease occurs quite consistently around the 10th-14th day after the appearance of the first symptoms of the disease, which is in correlation with the appearance of the first specific immunoglobulins against SARS-CoV-2 in the blood [39]. This fact leads to consider that the adaptive immune response with production of antibodies and expansion of T lymphocytes specific for the virus may be responsible for the observed symptoms. In the course of many infectious diseases, including influenza [46], and in sepsis [47],

an excess of immune response associated with a direct stimulation of pathogens can
cause the secretion of many inflammatory cytokines that interfere with the normal
evolution of the inflammatory response, resulting in local and systemic damage. In
such cases, more serious pathological changes are observed, such as diffuse alveolar
damage, formation of hyaline membranes, fibrin exudates and healing with fibrotic
outcomes. Signs of severe capillary damage, immunopathological lesions and or-
gan dysfunction can be added. In addition, inflammatory cytokines / chemokines
from the initial site can be released into the circulatory system and cause systemic
cytokine storms that are responsible for the dysfunction of many organs. During
Covid-19, the excess inflammatory response could be caused by a particularly vig-
orous secondary immune response and intense viral replication, with the release of
high amounts of viral antigens. This could happen due to a lack of initial control
of viral replication by the innate immune system and rapid colonization of the pul-
monary alveoli [39]. The alveoli, in fact, are anatomically predisposed sites for gas
exchange and do not have a strong natural immune defense against viruses. The
immunoglobulins that can be found are mainly those of the memory that exude
from the circulatory system due to inflammation, but the presence of natural im-
munoglobulins has not been described. An excess of specific cells could therefore
condition a greater production of inflammatory cytokines and the excess quantity
of antibodies could favor the formation and deposition of immune complexes which
contribute to the cytokine storm. The knowledge of the phenomenon of the cy-
tokine storm is important in order to implement the therapeutic approaches aimed
at mitigating its consequences.

Chapter 4

An introduction to the theory of the Boltzmann equation

4.1 Equivalence between kinetic formulation and scattering kernel formulation

The evolution equation for the one particle distribution function $f(x,\boldsymbol{\xi},t)$ of monoatomic rarefied gas was proposed in 1872 by Boltzmann [48]. The equation expresses the mass balance (conservation of mass) as a result of free flow and binary collision in the following form:

$$\frac{\partial f(x,\boldsymbol{\xi},t)}{\partial t} + \boldsymbol{\xi} \cdot \frac{\partial f(x,\boldsymbol{\xi},t)}{\partial x} = Q(f,f) \tag{4.1}$$

where $\boldsymbol{\xi}$ represents the velocity of the gas and $Q(f,f)$ is the collision operator, i.e. the operator that describes the interaction between two colliding molecules.

For a monatomic gas, one can prove the equivalence of the following formulations of the Boltzmann collision operator [49], [50].

(a) **Kinetic formulation**:

$$Q(f,f) = \int_{\mathbb{R}^3} d\mathbf{w} \int_{4\pi} g\,I(g,\boldsymbol{\chi})\,[f(\mathbf{v}')f(\mathbf{w}') - f(\mathbf{v})f(\mathbf{w})]\,d\hat{\Omega}' \tag{4.2}$$

where the post-collisional velocities $\mathbf{v}, \mathbf{w}$ and the pre-collisional velocities $\mathbf{v}', \mathbf{w}'$ are related through

$$\begin{cases} \mathbf{v}' = \mathbf{G} + \frac{1}{2} g \, \hat{\Omega}' \\ \mathbf{w}' = \mathbf{G} - \frac{1}{2} g \, \hat{\Omega}' \end{cases} \qquad (4.3)$$

with

$$\mathbf{G} = \frac{1}{2}(\mathbf{v} + \mathbf{w}) = \frac{1}{2}(\mathbf{v}' + \mathbf{w}')$$

being the velocity of the center of mass of the two colliding molecules, and

$$g = |\mathbf{v} - \mathbf{w}| = |\mathbf{v}' - \mathbf{w}'|$$

being the common modulus of the relative velocities. The deflection angle of the relative motion

$$\chi = \arccos(\hat{\Omega} \cdot \hat{\Omega}')$$

with

$$\hat{\Omega} = \frac{(\mathbf{v} - \mathbf{w})}{g}; \qquad \hat{\Omega}' = \frac{(\mathbf{v}' - \mathbf{w}')}{g'}$$

has been used as independent variable to account for the angular dependence of the differential scattering cross section $I(g, \chi)$.

If the collision of the molecules is deterministic (Eq. (4.3)), then the post-collisional velocities $\mathbf{v}, \mathbf{w}$ and the pre-collisional velocities $\mathbf{v}', \mathbf{w}'$ are related through the conservation laws (momentum and energy).

$$v + w = v' + w' \qquad \text{(momentum)} \qquad (4.4)$$

$$v^2 + w^2 = v'^2 + w'^2 \qquad \text{(energy)} \qquad (4.5)$$

If momentum and/or energy are not preserved, then the scattering process is called stochastic.

(b) **Scattering kernel formulation**:

$$Q(f, f) = \int_{\mathbb{R}^3} \int_{\mathbb{R}^3} \eta(\mathbf{v}', \mathbf{w}') A(\mathbf{v}', \mathbf{w}'; \mathbf{v}) f(\mathbf{v}') f(\mathbf{w}') \, d\mathbf{v}' \, d\mathbf{w}' - f(\mathbf{v}) \int_{\mathbb{R}^3} \eta(\mathbf{v}, \mathbf{w}) f(\mathbf{w}) \, d\mathbf{w}$$

$$(4.6)$$

where the scattering collision frequency is given by

$$\eta(\mathbf{v}, \mathbf{w}) =: \int_{\mathbb{R}^3} \int_{\mathbb{R}^3} \frac{1}{g} I(g, \chi) \, \delta(\mathbf{G} - \mathbf{G}') \, \delta(g - g') \, d\mathbf{v}' \, d\mathbf{w}' \qquad (4.7)$$

and

$$\eta(\mathbf{v}', \mathbf{w}') A(\mathbf{v}', \mathbf{w}'; \mathbf{v}) =: \int_{\mathbb{R}^3} \frac{1}{g} I(g, \chi) \, \delta(\mathbf{G} - \mathbf{G}') \, \delta(g - g') \, d\mathbf{w} \qquad (4.8)$$

For Maxwell molecules:

$$\eta = 4\pi k_s \qquad (4.9)$$

where k_s is a constant and

$$A(\mathbf{v}', \mathbf{w}'; \mathbf{v}) = \frac{\alpha_s(\chi^*)}{\pi g'} \delta(v^2 - (\mathbf{v}' + \mathbf{w}') \cdot \mathbf{v} + \mathbf{v}' \cdot \mathbf{w}') \qquad (4.10)$$

where

$$\cos(\chi^*) = \frac{2\mathbf{v} \cdot (\mathbf{v}' - \mathbf{w}') - v'^2 + w'^2}{|\mathbf{v}' - \mathbf{w}'|^2}$$

with α_s being a suitable function of χ^*. Under the additional assumption of isotropic scattering, α_s becomes a constant equal to 1.

The scattering kernel formalism remains valid also with stochastic collisions, and, it was proven in [49], [50] that, it is indeed equivalent with the kinetic formulation in the deterministic case (Eqs. (4.7)-(4.8)). For stochastic models, in which $A(\mathbf{v}', \mathbf{w}'; \mathbf{v})$ satisfies only the relationships

$$A(\mathbf{v}', \mathbf{w}'; \mathbf{v}) = A(\mathbf{w}', \mathbf{v}'; \mathbf{v}) \qquad \text{(symmetry property)} \qquad (4.11)$$

$$\int_{\mathbb{R}^3} A(\mathbf{v}', \mathbf{w}'; \mathbf{v}) \, d\mathbf{v} = 1 \qquad \text{(normalization property)} \qquad (4.12)$$

with $\mathbf{v}', \mathbf{w}', \mathbf{v}$ independent velocities, one cannot expect conservation of momentum and energy.

4.2   Reactive gas mixtures

Let us consider a mixture of four gas species which, besides all elastic collisions, can interact according to the following reversible bimolecular reaction:

$$1+2 \rightleftarrows 3+4. \tag{4.13}$$

When a particle j, of velocity $\mathbf{w}$, collides with a particle i, of velocity $\mathbf{v}$, the relative velocity can be written as

$$\mathbf{w} - \mathbf{v} = V \hat{\Omega} \tag{4.14}$$

with $V = |\mathbf{w} - \mathbf{v}|$ and $|\hat{\Omega}| = 1$. If the collision yields a pair of molecules h, k with velocities $\mathbf{v}'$ and $\mathbf{w}'$, respectively, the differential scattering cross section is labeled by I_{ij}^{hk}. Let us also introduce the symbols m_i and E_i, which stand for particle mass and internal energy of chemical bond, respectively. Furthermore, we assume that the chemical reaction is affected by an energy threshold (activation energy):

$$\Delta E = E_3 + E_4 - E_1 - E_2 \geq 0. \tag{4.15}$$

By adding the contribution of both elastic and chemical interactions, the kinetic equations (of the Boltzmann type) read as

$$\frac{\partial f_s}{\partial t}(t, \mathbf{v}) = \sum_{r=1}^{4} Q^{sr} + \overline{Q}^s \qquad s = 1, \ldots, 4. \tag{4.16}$$

In Eq. (4.16), Q^{sr} is the elastic collision operator for the binary (s, r) interaction given by

$$Q^{sr} = \int d\mathbf{w} \int V I_{sr}^{sr}(V, \hat{\Omega} \cdot \hat{\Omega}') \left[f_s(\mathbf{v}') f_r(\mathbf{w}') - f_s(\mathbf{v}) f_r(\mathbf{w}) \right] d\hat{\Omega}' \tag{4.17}$$

where the post-collisional velocities can be written as

$$\begin{cases} \mathbf{v}' = \dfrac{[m_s \mathbf{v} + m_r \mathbf{w} - m_r V \hat{\Omega}']}{(m_s + m_r)} \\[4mm] \mathbf{w}' = \dfrac{[m_s \mathbf{v} + m_r \mathbf{w} + m_s V \hat{\Omega}']}{(m_s + m_r)} \end{cases} \tag{4.18}$$

with $\hat{\Omega}' = \dfrac{\mathbf{w}' - \mathbf{v}'}{|\mathbf{w}' - \mathbf{v}'|}$.

If the microreversibility of reaction is invoked, the chemical collision term $\overline{Q}^s$ in Eq. (4.16) reads:

$$\overline{Q}^1 = \int_{\mathbb{R}^3} \int_{4\pi} H(V^2 - \frac{2\Delta E}{\mu^{12}}) V I_{12}^{34}(V, \hat{\Omega} \cdot \hat{\Omega}') \left[\left(\frac{\mu^{12}}{\mu^{34}} \right)^3 f_3(\mathbf{v}') f_4(\mathbf{w}') - f_1(\mathbf{v}) f_2(\mathbf{w}) \right] d\mathbf{w} \, d\hat{\Omega}'$$

$$(4.19)$$

where μ^{sr} denotes the reduced mass of the (s, r) pair:

$$\mu^{sr} = \frac{m_s m_r}{(m_s + m_r)}$$

and H is the Heaviside function, which accounts for the fact that the reaction cannot occur if a threshold is not overcome. For species 3, the calculation proceeds in exactly the same way, with the only important difference that particles 3 and 4 may collide whatever their relative speed (loss term), or are produced with unrestricted relative speed (gain term):

$$\overline{Q}^3 = \int_{\mathbb{R}^3} \int_{4\pi} V I_{34}^{12}(V, \hat{\Omega} \cdot \hat{\Omega}') \left[\left(\frac{\mu^{34}}{\mu^{12}} \right)^3 f_1(\mathbf{v}') f_2(\mathbf{w}') - f_3(\mathbf{v}) f_4(\mathbf{w}) \right] d\mathbf{w} \, d\hat{\Omega}' \qquad (4.20)$$

Collision terms for species 2 and 4 are analogously calculated by suitable permutations of indices [53].

Chapter 5

Microscopic models for the large-scale spread of SARS-CoV-2: A Statistical Mechanics approach

5.1 Mathematical formulation

We derive a model describing the spread of SARS-CoV-2 virus within the general mathematical framework of the kinetic theory for chemically reacting mixtures of gases. The system consists of two populations of interacting individuals. Each population is denoted by the subscript i $(i = 1, 2)$, according to the following classification:

$$\begin{cases} i = 1: & \text{susceptible individuals} \\ i = 2: & \text{infected individuals.} \end{cases} \qquad (5.1)$$

Within the same population, each individual is characterized by a microscopic state, which is a scalar variable $u \in (-\infty, +\infty)$, called *activity* [51], [52]. Let us introduce the one-particle distribution function: $f_i = f_i(t, u)$. By definition, the product

$$f_i(t, u)\, du$$

gives the number of individuals of the i-th population which at the time t are in the elementary state $[u, u + du]$. The variable u depends on the intensity level of a certain pathological state. We distinguish the following cases:

$$f_1(t, u_1) : \begin{cases} \text{if } u_1 < 0 & \rightarrow \text{ healthy-individuals} \\ \text{if } u_1 \geq 0 & \rightarrow \text{ positive-asymptomatic} \end{cases} \tag{5.2}$$

$$f_2(t, u_2) : \begin{cases} \text{if } u_2 < 0 & \rightarrow \text{ positive-symptomatic} \\ \text{if } u_2 \geq 0 & \rightarrow \text{ hospitalized-individuals.} \end{cases} \tag{5.3}$$

Specifically, within the same population, the larger is the value of u_i, the stronger is the infection.

The evolution of the system is determined by microscopic interactions between pairs of individuals, which modify the probability distribution over the state variable and/or the size of the population. The system is homogeneous in space and only binary interactions are taken into account. In addition, we model also the action of the immune system described by the distribution function $\phi_i(v)$ $(i = 1, 2)$ over the microscopic variable $v \in (-\infty, +\infty)$. The immune response to SARS-CoV-2 virus is unpredictable and very different from person to person. We distinguish between two natural actions, according to Sec. (3.0.2):

(i) The innate immunity represented by the distribution function $\phi_1(v)$.

Bacteria or viruses that enter the body can be stopped right away by the innate immune system. The effectiveness of this type of action is linked to the possibility that an individual belonging to population 1 becomes ill or not.

(ii) The adaptive immunity represented by the distribution function $\phi_2(v)$.

The adaptive immune system takes over if the innate immune system is not able to destroy the germs. It is slower to respond than the innate immune system, but it identifies the germs and it is able to "remember" them. The recovery of an individual belonging to population 2, who has been sick even in the absence of a specific care, can be ascribed to the adaptive immunity. On the contrary, the hyperactivation of the immune system, and subsequent exacerbated systemic inflammatory response, can lead to a major complication of Covid-19 disease.

We will consider the following moments of the distribution functions.

(a) The size of the i-th population at time t correspond to the mean of the distribution function f_i over the microscopic state variable u_i:

$$n_i(t) = \int_{\mathbb{R}} f_i(t, u_i)\, du_i, \quad i = 1, 2. \tag{5.4}$$

The total number of individuals at time t is given by the sum of the sizes of the single populations:

$$N(t) = \sum_{i=1}^{2} n_i(t). \tag{5.5}$$

Since we are dealing with an epidemic, which outbreak is really rapid and occurs within less than one year, we can assume conservation holds. It implies:

$$\sum_{i=1}^{2} n_i(t) = 1. \tag{5.6}$$

(b) The average amount of the action of the immune system on the individuals of the i-th population is given by the mean of the distribution function over the microscopic variable v:

$$\hat{I}_i = \int_{\mathbb{R}} \phi_i(v)\, dv, \quad i = 1, 2. \tag{5.7}$$

(c) The progression of the epidemiological state is defined as the first moment:

$$a_i(t) = \int_{\mathbb{R}} u_i\, f_i(t, u_i)\, du_i \quad i = 1, 2 \tag{5.8}$$

which represents the mean value of the activity variable of the i-th population.

Higher-order moments provide additional information on the (macroscopic) description of the system.

The evolution equations for the distribution functions $f_i(t, u_i)$ can be obtained following the formalism of the Boltzmann equations for chemically reacting gas mixtures (see Chapter 3 Section 4.2). In order to derive these equations, we consider the following hypotheses on interaction processes.

(H.1) The medical staff belongs to the population 1, with $u_1 \in [-\infty, 0)$.

(H.2) The interactions produce a smooth shift towards higher pathological states
(e.g., a healthy person does not immediately become ill but positive-asymptomatic).

(H.3) All positive-symptomatic individuals are in isolation and, therefore, they can
only have interactions with family members and medical staff.

(H.4) Hospitalized-individuals can only have interactions between themselves and
with the medical staff. This type of encounter could possibly allow infected
population to recover thanks to the health cares.

Relying on these assumptions, we describe the interactions within the same population or between different populations as follows.

Interactions within the population 1:

(a)   *Healthy-individuals + healthy-individuals ⟶ healthy-individuals* (stay in population 1).

Two healthy individuals who meet can modify their microscopic status without moving into a different population.

(b) *Healthy-individuals + positive-asymptomatic ⟶ positive-asymptomatic* (stay in population 1).

An healthy individual who meet a positive-asymptomatic can be infected and become a positive asymptomatic as well. This implies a change in the activity variable but not a transition into population 2.

(c) *Positive-asymptomatic + positive-asymptomatic ⟶ positive-asymptomatic + positive-symptomatic* (transition to population 2).

Two positive asymptomatic who interact can become symptomatic and pass to the infected population 2.

Interactions within the population 2:

(d) *Positive-symptomatic + positive-symptomatic ⟶ positive-symptomatic + hospitalized-individuals* (stay in population 2).

The contact between two positive symptomatic individuals could make the viral load increase, worsening the health condition of one among them and leading him/her in the hospitalized population.

(e) *Hospitalized-individuals + hospitalized-individuals* $\longrightarrow$ *hospitalized-individuals*
(stay in population 2).

Two hospitalized individuals can interact changing their status without transition to population 1.

Interactions between the populations 1 and 2:

(f) *Healthy-individuals (medical staff) + positive-symptomatic* $\longrightarrow$ *healthy-individuals* (transition to population 1).

The interaction between the medical staff and positive symptomatic individuals could bring the latter to population 1 thanks to health cares and their recovery.

(g) *Healthy-individuals (medical staff) + hospitalized-individuals* $\longrightarrow$ *healthy - individuals* (transition to population 1).

The interaction between a medical staff member and a hospitalized individual takes into consideration the intensive cares a Covid-19 sick person receives in the intensive care unit, which allow him/her to recover and go back to the healthy population.

(h) *Healthy-individuals (medical staff) + hospitalized-individuals* $\longrightarrow$ *healthy- individuals + hospitalized-individuals* (stay in their respective population).

The interaction between a medical staff member and a hospitalized individual that is not sufficient to allow the sick person to recover.

Therefore, we shall deal with a "mixture" of two populations $(1, 2)$ which can interact according to the following reversible "chemical reaction":

$$1 + 1 \rightleftarrows 2 + 1 \tag{5.9}$$

In addition to the interactions between individuals, we consider also those between an individual and the immune system.

In the following, we consider the scattering kernel formulation of the Boltzmann collision operator for both "elastic" (Q_{hk}) and "chemical" interactions $(\overline{Q}_i^{(r)}, \overline{L}_i^{(r)})$.

Elastic terms take into consideration all the interactions that do not imply a transfer between populations but only a variation in the microscopic state u_i (such as interactions (a), (b), (d), (e), (h)). Chemical terms instead describe the interactions that entail transition from a population to the other (see interactions (c), (f), (g)). In particular, we obtain the following evolution equation for the distribution density function of population 1 with microscopic activity u_1 :

$$\frac{\partial f_1}{\partial t}(t, u_1) = Q_{11} + Q_{12} + \overline{Q}_1^{(r)} + \overline{L}_1^{(r)} \tag{5.10}$$

where each term on the right-hand side can be written as the difference between a gain and a loss contribution as follows.

(i) The elastic term Q_{11}:

$$Q_{11} = \int_{\mathbb{R}} \int_{\mathbb{R}} \eta_{11}(u_*, u^*) A_{11}^{(1)}(u_*, u^*; u_1) f_1(t, u_*) f_1(t, u^*) du_* du^*$$
$$- f_1(t, u_1) \int_{\mathbb{R}} \eta_{11}(u_1, u^*) f_1(t, u^*) du^* \tag{5.11}$$

This term represents the encounter between two individuals belonging to population 1 i.e. healthy or positive asymptomatic. The gain term represents an individual whose microscopic state takes value u_1, while the loss term describes an individual whose microscopic state, that previously had value u_1, changes due to the interaction.

(ii) The elastic contribution Q_{12}:

$$Q_{12} = \int_{\mathbb{R}} \int_{\mathbb{R}} \eta_{12}(u_*, u^*) A_{12}^{(1)}(u_*, u^*; u_1) f_1(t, u_*) f_2(t, u^*) du_* du^*$$
$$- f_1(t, u_1) \int_{\mathbb{R}} \eta_{12}(u_1, u^*) f_2(t, u^*) du^* \tag{5.12}$$

which describes the interactions of individuals of population 1 and population 2, leaving the people in their original classes. The gain term represents the case of the interaction between a medical staff member, whose status takes value u_1, and an hospitalized patient who does not recover. The loss term instead describes the case of a medical staff member who changes the microscopic state is u_1 after the encounter with a sick patient.

(iii) The reactive chemical contribution $\overline{Q}_1^{(r)}$:

$$
\overline{Q}_1^{(r)} = \int_{\mathbb{R}} \int_{\mathbb{R}} \eta_{21}^{(r)}(u_*, u^*) A_{21}^{(1)}(u_*, u^*; u_1) f_2(t, u_*) f_1(t, u^*) \, du_* \, du^*
$$
$$
- f_1(t, u_1) \int_{\mathbb{R}} \eta_{11}^{(r)}(u_1, u^*) f_1(t, u^*) \, du^* \tag{5.13}
$$

In the gain term of $\overline{Q}_1^{(r)}$ it is contained the recovery due to the response to specific treatments that work, while in the loss term there is the possibility that in the encounter between two asymptomatic patients, one becomes sick because his/her viral load increases due to transmission of viral load by the other individual.

(iv) The linear reactive chemical term $\overline{L}_1^r$:

$$
\overline{L}_1^{(r)} = \int_{\mathbb{R}} \int_{\mathbb{R}} \mu_2^{(r)}(u_*, v^*) B_2^{(1)}(u_*, v^*; u_1) f_2(t, u_*) \phi_2(v^*) \, du_* \, dv^*
$$
$$
- f_1(t, u_1) \int_{\mathbb{R}} \mu_1^{(r)}(u_1, v^*) \phi_1(v^*) \, dv^* \tag{5.14}
$$

which describes the interaction of an individual with his/her immune system, described by the function ϕ_1 and ϕ_2. In the gain term of $\overline{L}_1^{(r)}$ it is contained the healing obtained "by chance", i.e. for an optimal response of the organism to the virus (even in the absence of specific treatments), while the loss term contains the possibility that an asymptomatic positive will fall ill due to an adverse reaction of his body to the virus.

The distribution functions describing the action of the immune system ϕ_1 and ϕ_2 are different because of the different immunological response to the infection, which could be either innate or adaptive (see Sec. (3.0.2)).

Likewise, we can write for population 2, with microscopic state variable u_2, the following evolution equation:

$$
\frac{\partial f_2}{\partial t}(t, u_2) = Q_{22} + Q_{21} + \overline{Q}_2^{(r)} + \overline{L}_2^{(r)} \tag{5.15}
$$

where, as before, each term on the tight hand-side can be written as the difference of two contribution.

(i) The elastic term Q_{22}:

$$Q_{22} = \int_{\mathbb{R}} \int_{\mathbb{R}} \eta_{22}(u_*, u^*) A_{22}^{(2)}(u_*, u^*; u_2) f_2(t, u_*) f_2(t, u^*) \, du_* \, du^*$$
$$- f_2(t, u_2) \int_{\mathbb{R}} \eta_{22}(u_2, u^*) f_2(t, u^*) \, du^* \tag{5.16}$$

This term describes the interactions between two symptomatic-positive or hospitalized individuals. The microscopic state of one of them could take value u_2 or, if it previously had value u_2, change it.

(ii) The elastic term Q_{12}:

$$Q_{21} = \int_{\mathbb{R}} \int_{\mathbb{R}} \eta_{21}(u_*, u^*) A_{21}^{(2)}(u_*, u^*; u_2) f_2(t, u_*) f_1(t, u^*) \, du_* \, du^*$$
$$- f_2(t, u_2) \int_{\mathbb{R}} \eta_{21}(u_2, u^*) f_1(t, u^*) \, du^* \tag{5.17}$$

which describes the interaction of a medical staff member, of population 1, and a sick person, of population 2. Here the microscopic state of the infected person can take value u_2 or, if it previously had value u_2, change it, but no one gets sick or recovers.

(iii) The reactive chemical term $\overline{Q}_2^{(r)}$:

$$\overline{Q}_2^{(r)} = \int_{\mathbb{R}} \int_{\mathbb{R}} \eta_{11}^{(r)}(u_*, u^*) A_{11}^{(2)}(u_*, u^*; u_2) f_1(t, u_*) f_1(t, u^*) \, du_* \, du^*$$
$$- f_2(t, u_2) \int_{\mathbb{R}} \eta_{21}^{(r)}(u_2, u^*) f_1(t, u^*) \, du^*. \tag{5.18}$$

In the gain term of $\overline{Q}_2^{(r)}$ it is contained the possibility that in the encounter between two asymptomatic patients, one becomes sick because his/her viral load increases due to transmission. In the loss term instead the possibility of recovery due to specific treatments that work is considered.

(iv) The reactive chemical term $\overline{L}_2^{(r)}$:

$$\overline{L}_2^{(r)} = \int_{\mathbb{R}} \int_{\mathbb{R}} \mu_1^{(r)}(u_*, v^*) B_1^{(2)}(u_*, v^*; u_2) f_1(t, u_*) \phi_1(v^*) \, du_* \, dv^*$$
$$- f_2(t, u_2) \int_{\mathbb{R}} \mu_2^{(r)}(u_2, v^*) \phi_2(v^*) \, dv^*. \tag{5.19}$$

which represents the action of the innate or adaptive immune system through ϕ_1 and ϕ_2 respectively. In the gain term of $\overline{L}_2^{(r)}$ it is contained the possibility that an

asymptomatic positive will fall ill due to an adverse reaction of his body to the virus, while the loss term describes the healing obtained "by chance", i.e. for an optimal response of the organism to the virus (even in the absence of specific treatments).

In the above equations, η_{hk} is called *encounter rate* and it describes the rate of interactions, i.e. the number of encounters per unit time, between individuals of the h-th population and individuals of the k-th population, while $\mu_h^{(r)}$ refers to the rate of interaction between individuals of the h-th population and the immune system. The modification of the state of interacting individuals of the same or different population is described by the transition probability density, $A_{hk}^{(i)}(u_*, u^*; u_i)$, of individuals which are shifted into the i-th population with state u_i due to encounters between an individual of the h-th population in the state u_* with an individual of the k-th population in the state u^*. Likewise, $B_h^{(i)}(u_*, v^*; u_i)$ represents the transition probability density of individuals which are shifted into the i-th population with state u_i due to the interaction between an individual of the h-th population in the state u_* with the immune system characterized by the microscopic state v^*.

We further define $T_{hk}^{(i)}(u_*, u^*; u_i)$ and $S_h^{(i)}(u_*, v^*; u_i)$ as the *transition rates* into population i caused by the encounter between two individual of the h-th and k-th populations in the first case, and caused by an individual of the h-th population and the immune system in the second one. These rates correspond to the product between the encounter/interaction rate and the transition probability function:

$$T_{hk}^{(i)}(u_*, u^*; u_i) = \eta_{hk}(u_*, u^*)\, A_{hk}^{(i)}(u_*, u^*; u_i) \qquad h, k, i = 1, 2, \qquad (5.20)$$

$$S_h^{(i)}(u_*, v^*; u_i) = \mu_h^{(r)}(u_*, v^*)\, B_h^{(i)}(u_*, v^*; u_i) \qquad h, i = 1, 2. \qquad (5.21)$$

For stochastic models of interaction between individuals, the transition probability density $A_{hk}^{(i)}$ satisfies the following properties:

(i) Symmetry property

$$A_{hk}^{(i)}(u_*, u^*; u_i) = A_{kh}^{(i)}(u^*, u_*; u_i) \quad \forall\, h, k, i \qquad (5.22)$$

expressing indistinguishability of individuals;

(ii) Normalization property

$$\int du_i A^{(i)}_{hk}(u_*, u^*; u_i) = 1 \quad \forall\, h, k, i. \tag{5.23}$$

We assume that also the probability density $B^{(i)}_h$ is normalized with respect to all possible final states:

$$\int du_i B^{(i)}_h(u_*, v^*; u_i) = 1 \quad \forall\, h, i. \tag{5.24}$$

Stochastic models, describing the interactions within each population, have been proposed in order to give an explicit expression for the transition probability $A^{(i)}_{hk}$ in the collisional operator of the Boltzmann equation (Eqs. (5.10), (5.15)). In particular, the interactions within the population 1, taken into account by the term Q_{11}, can be modeled as follows:

$$\begin{cases} u'_* &= \frac{1}{2}(u_* + u^*) + \tilde{\eta} u_* \\ u'^* &= \frac{1}{2}(u_* + u^*) + \eta u^* \end{cases} \tag{5.25}$$

where (u_*, u^*) and (u'_*, u'^*) denote the infectious states of two individuals before and after their encounter, respectively. In Eq. (5.25), η and $\tilde{\eta}$ are positive random variables characterized by the exponential distribution with mean $1/\lambda$ and variance $1/\lambda^2$ (where $\lambda > 0$ is the parameter of the distribution, called the rate parameter). To reproduce the interactions described in the term Q_{11}, we have chosen a high value of λ so that the expectation values of η and $\tilde{\eta}$ lie close to zero. Likewise, we can write for the interaction rules underlying the transition probabilities in the term Q_{22}:

$$\begin{cases} u'_* &= \frac{1}{2}(u_* + u^*) \mp \tilde{\mu} u_* \\ u'^* &= \frac{1}{2}(u_* + u^*) \mp \mu u^* \end{cases} \tag{5.26}$$

where the minus sign refers to the interaction between two positive-symptomatic individuals, while the plus sign refers to the interaction between two hospitalized-individuals. Again, μ and $\tilde{\mu}$ are positive random variables characterized by the exponential distribution with an expectation value greater than 1. To model the interaction rules involved in the term Q_{12} (or Q_{21}), we can use the system (5.25), but

in this case the exponential distribution for the random variables η and $\tilde{\eta}$ should
have an expectation value greater than 1.

To construct the transition rates, we assume that the interactions between individuals can be modeled in analogy to the intermolecular potentials acting between
the gas molecules. Since in the framework of kinetic theory of rarefied gases analytical manipulations can be carried out in closed form for Maxwell molecules, we
restrict ourselves to this kind of interaction, characterized by the following interparticle force law:

$$F^{hk} = \frac{K^{hk}}{r_d^5} \tag{5.27}$$

(where r_d is the distance between particles and K^{hk} is the interparticle force law
constant).

Concerning the interactions between individuals, in analogy with the Maxwell molecules
in the framework of rarefied gas dynamics, we can assume that:

$$\eta_{hk} = const \qquad h,k = 1,2. \tag{5.28}$$

For sake of simplicity we also assume: $\mu_h^{(r)} = const \quad h = 1,2$.

In order to derive the macroscopic equations for the evolution of the size of the two
populations, we have to integrate Eq. (5.10) by u_1 and Eq. (5.15) by u_2.
Therefore, from Eq. (5.10) we get

$$\begin{aligned}
\frac{\partial n_1}{\partial t} &= \eta_{11} \int \int du_* \, du^* \left[\int du_1 A_{11}^{(1)}(u_*, u^*; u_1) \right] f_1(t, u_*) f_1(t, u^*) \\
&\quad -\eta_{11} n_1^2 + \eta_{12} \int \int du_* \, du^* \left[\int du_1 A_{12}^{(1)}(u_*, u^*; u_1) \right] f_1(t, u_*) f_2(t, u^*) \\
&\quad -\eta_{12} n_1 n_2 + \eta_{21}^{(r)} \int \int du_* \, du^* \left[\int du_1 A_{21}^{(1)}(u_*, u^*; u_1) \right] f_2(t, u_*) f_1(t, u^*) - \eta_{11}^{(r)} n_1^2 \\
&\quad +\mu_2^{(r)} \int \int du_* \, dv^* \left[\int du_1 B_2^{(1)}(u_*, v^*; u_1) \right] f_2(t, u_*) \phi_2(v^*) - \mu_1^{(r)} n_1 \hat{I}_1.
\end{aligned} \tag{5.29}$$

By using the properties (5.23) and (5.24) of the transition probability densities, Eq.
(5.29) becomes:

$$\frac{\partial n_1}{\partial t} = \eta_{21}^{(r)} n_1 n_2 - \eta_{11}^{(r)} n_1^2 + \mu_2^{(r)} n_2 \hat{I}_2 - \mu_1^{(r)} n_1 \hat{I}_1. \tag{5.30}$$

From Eq. (5.15) we get

$$
\frac{\partial n_2}{\partial t} = \eta_{22} \int\int du_* \, du^* \left[\int du_2 A_{22}^{(2)}(u_*,u^*;u_2) \right] f_2(t,u_*) \, f_2(t,u^*)
$$

$$
- \eta_{22} \, n_2^2 + \eta_{21} \int\int du_* \, du^* \left[\int du_2 A_{21}^{(2)}(u_*,u^*;u_2) \right] f_2(t,u_*) \, f_1(t,u^*)
$$

$$
- \eta_{21} \, n_2 \, n_1 + \eta_{11}^{(r)} \int\int du_* \, du^* \left[\int du_2 A_{11}^{(2)}(u_*,u^*;u_2) \right] f_1(t,u_*) \, f_1(t,u^*) - \eta_{21}^{(r)} \, n_2 \, n_1
$$

$$
+ \mu_1^{(r)} \int\int du_* \, dv^* \left[\int du_2 B_1^{(2)}(u_*,v^*;u_2) \right] f_1(t,u_*) \, \phi_1(v^*) - \mu_2^{(r)} \, n_2 \, \hat{I}_2. \quad (5.31)
$$

By using the properties (5.23) and (5.24) of the transition probability densities, Eq. (5.31) becomes:

$$
\frac{\partial n_2}{\partial t} = \eta_{11}^{(r)} \, n_1^2 - \eta_{21}^{(r)} \, n_2 \, n_1 + \mu_1^{(r)} \, n_1 \, \hat{I}_1 - \mu_2^{(r)} \, n_2 \, \hat{I}_2. \quad (5.32)
$$

One can easily check from Eqs. (5.29)-(5.32) that the conservation laws are satisfied for both the 'elastic' and the 'chemical' collision operators, respectively:

$$
\int Q_{hk}(u) \, du = 0 \quad \forall h,k \quad (5.33)
$$

$$
\int \overline{Q}_1^{(r)} \, du + \int \overline{Q}_2^{(r)} \, du = 0. \quad (5.34)
$$

$$
\int \overline{L}_1^{(r)} \, du + \int \overline{L}_2^{(r)} \, du = 0. \quad (5.35)
$$

Theorem 5.1.1 (Existence and uniqueness of solution)**.**

Let $\boldsymbol{f}_0 = (f_{01}, f_{02}) \in X^+ = \{\boldsymbol{h} = (h_1, h_2) \in X \mid h_i \geq 0, i = 1,2\}$ *where* $X = [L^1(\mathbb{R})]^2$, $\boldsymbol{g} = (g_1, g_2)$ *where* $g_i \in L^1(\mathbb{R}_0^+) \cap L^1(\mathbb{R}_0^+)$ *for* $i = 1,2$, $\phi_i \in L^1(\mathbb{R}_0^+) \cap L^1(\mathbb{R}_0^+)$ *for* $i = 1,2$, $\eta_{hk} = const$ *and* $\mu_h^{(r)} = const$ $\forall h,k$ *and,* $A_{hk}^{(i)}$ *and* $B_h^{(i)}$ *continuous and bounded satisfying (5.23) and (5.24). Then for any positive constant* $\boldsymbol{t}$ *the initial value problem:*

$$
\begin{cases} \dfrac{\partial \boldsymbol{f}}{\partial t} = \boldsymbol{K}[\boldsymbol{f}, \boldsymbol{g}] \\[2mm] \boldsymbol{f}(t=0,u) = \boldsymbol{f}_0(u) \end{cases} \quad (5.36)
$$

where $\boldsymbol{K}[\boldsymbol{f}, \boldsymbol{g}] = (K_1[\boldsymbol{f}, \boldsymbol{g}], K_2[\boldsymbol{f}, \boldsymbol{g}])$ *with* K_1 *and* K_2 *defined in (5.10) and (5.15),*

i.e. $K_1[\boldsymbol{f}, \boldsymbol{g}] = Q_{11} + Q_{12} + \overline{Q}_1^{(r)} + \overline{L}_1^{(r)}$ *and* $K_2[\boldsymbol{f}, \boldsymbol{g}] = Q_{22} + Q_{21} + \overline{Q}_2^{(r)} + \overline{L}_2^{(r)}$ *with the relative terms defined in (5.11), (5.12), (5.13), (5.14), (5.16), (5.17), (5.18) and (5.19).*

Then (5.36) has a unique solution $\boldsymbol{f} \in Y^+ = \mathbf{C}([0,T], X^+)$.

Indeed the solution satisfies $\boldsymbol{f}(t) \in X^+, t \in [0,T]$ *and moreover is* $||\boldsymbol{f}|| = ||\boldsymbol{f}_0||$.

Proof. The transition rate operators

$$T_{hk}^{(i)}(u_*, u^*; u_i) = \eta_{hk}(u_*, u^*) A_{hk}^{(i)}(u_*, u^*; u_i) \qquad h, k, i = 1, 2, \tag{5.37}$$

$$S_h^{(i)}(u_*, v^*; u_i) = \mu_h^{(r)}(u_*, v^*) B_h^{(i)}(u_*, v^*; u_i) \qquad h, i = 1, 2. \tag{5.38}$$

are continuous and bounded over the domain of the microscopic states thanks to the assumptions on the probability density $A_{hk}^{(i)}$ and $B_h^{(i)}$.

We want to apply the fixed point theorem on the cone Y and Y^+ in order to prove the local existence and positivity of a fixed point for the problem (5.36), which constitutes its solution. Exploiting (5.23), (5.24), (5.22) and the inequality $|n_i| = \left| \int_{-\infty}^{+\infty} f_i(t, u_i) du_i \right| \leq ||f_i|| \quad i = 1, 2$ we obtain that $\mathbf{K}$ is Lipschitz-continuous with constant C in Y:

$$||\mathbf{K}(\mathbf{f}_1, g) - \mathbf{K}(\mathbf{f}_2, g)|| \leq C ||\mathbf{f}_1 - \mathbf{f}_2||$$

Moreover, according to the same proof lines of Theorem 4.2.1. in Ref [54], we can prove that the operator $\mathbf{K}$ is a contraction and we can now apply the fixed point theorem on the positive cone Y^+ and asserting that there exists a unique local solution $\mathbf{f}(t) \in Y^+$ of the initial value problem (5.36) on $[0,T]$.

Moreover since we assume to deal with number conservative interactions, (see equation (1)), it follows that

$$\frac{\partial ||\mathbf{f}||_{Y^+}}{\partial t} = 0. \tag{5.39}$$

Furthermore we observe that

$$\frac{\partial ||\mathbf{f}||_{Y^+}}{\partial t} := \sup_{t \in [0,T]} \partial_t \left(\sum_{i=1,2} \int_{\mathbb{R}} f_i(t, u) du \right) = 0,$$

which implies

$$||\mathbf{f}||_{Y^+} = ||\mathbf{f}|| = ||\mathbf{f}_0||.$$

Finally by analytical prolongation it is possible to prove the global existence of the
solution of the (5.36). □

5.2 Correlation with SIS compartmental model

In the previous section (5.1) we have found that the evolution equations for the
population sizes n_1 and n_2 behave as

$$
\begin{cases}
\dfrac{\partial n_1}{\partial t} = \eta_{21}^{(r)} n_1 n_2 - \eta_{11}^{(r)} n_1^2 + \mu_2^{(r)} n_2 \hat{I}_2 - \mu_1^{(r)} n_1 \hat{I}_1. \\[3mm]
\dfrac{\partial n_2}{\partial t} = \eta_{11}^{(r)} n_1^2 - \eta_{21}^{(r)} n_2 n_1 + \mu_1^{(r)} n_1 \hat{I}_1 - \mu_2^{(r)} n_2 \hat{I}_2.
\end{cases}
\tag{5.40}
$$

We now consider:

- $n_1 = s(t)$ as the susceptible population density function, which comprehends
  both healthy and positive-asymptomatic individuals;

- $n_2 = i(t)$ as the infected population density function, which comprehends both
  positive-symptomatic and hospitalized individuals;

- $\eta_{11} = \beta$ as the contact rate, introduced in Sec. (2.2.1), between asymptomatic-
  positive individuals who arise their viral load enough to be transferred to the
  infected population 2;

- $\eta_{21} = \gamma$ as the recovery rate, introduced in Sec. (2.2.1), that allows an highly
  infected person to recover after the encounter with a medical staff member
  whose health cares are need for healing;

- $\mu_1^{(r)} \hat{I}_1 = \tau_i$ as the infection rate due to the weak response of the immune system
  of a susceptible individual;

- $\mu_2^{(r)} \hat{I}_2 = \tau_r$ as the recovery rate due to the action of the immune system of an
  infected individual.

This procedure leads to the following system:

$$
\begin{cases}
\dfrac{\partial s}{\partial t} = \gamma i(t)\,s(t) - \beta\,s(t)^2 + \tau_r\,i(t) - \tau_i\,s(t), \\[2mm]
\dfrac{\partial i(t)}{\partial t} = \beta\,s(t)^2 - \gamma i(t)\,s(t) + \tau_i\,s(t) - \tau_r\,i(t).
\end{cases}
\tag{5.41}
$$

This model corresponds to the SIS compartmental counterpart of out kinetic model
for SARS-CoV-2. Here both linear and quadratic contributions are exploited.
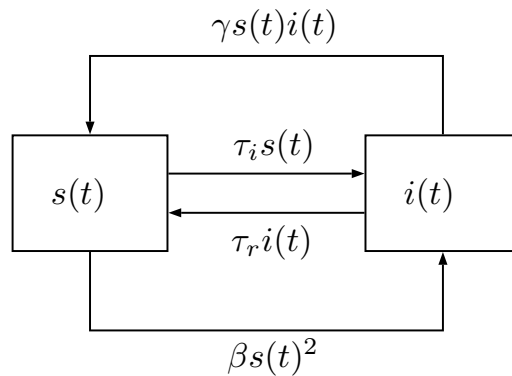
Figure 5.1: Flowchart of SIS-Kinetic model (5.41).

The mechanisms of contagion and recovery present differences between the basic SIS
endemic model. The main difference are:

1. In the basic SIS model the contagion occurs only by direct contact of two indi-
   viduals, while in our model contagion does not only take it into consideration,
   but it also relies on an "interaction potential" which allows to insert long-range
   interactions between individuals. This makes the model self-consistent and al-
   lows one to include the peculiarities of spread of SARS-CoV-2, such as the
   fact that the transmission spreads primarily by airway of aerosol particles and
   droplets and may occur by entering a room, or a place that is currently or has
   been occupied by an infective.

2. In the basic SIS model the mechanism of contagion entails that a sick person
   should have a direct contact with an healthy individual to infect him/her.
   Instead in the kinetic theory applied model contagion occurs in two different

ways. The first one describes the situation of two asymptomatic-positive indi-
viduals that increase their viral load and enter the infected population. This
fact allows us to deal only with smooth shifts towards higher pathological
states. The second one instead includes the circumstances of healthy individ-
uals whose immune system is not strong enough to prevent them to get sick.
This last case takes into consideration all that situations according to which
there is no contact and it is not clear who infects whom, such as traveling with
public transportation, being in places that have been infected by the presence
of sick people...

3. As for recovery, in basic SIS models what a person needs to recover is to just
   let an average period of $1/\tilde{\gamma}$ units of time pass (where $\tilde{\gamma}$ corresponds to the
   recovery rate γ of the model defined in Sec. (2.2.1)). In our model instead
   an interaction with a medical staff that gives the patient enough health treat-
   ments, such breathing tube, is required. Another way according to which an
   individual could heal takes into consideration the possibility that the infected
   recovers thanks to the response of his immune system.

We observe that conservation of total population size is satisfied:

$$\frac{\partial s(t)}{\partial t} + \frac{\partial i(t)}{\partial t} = \gamma s(t)\,i(t) - \beta\,s(t)^2 + \mu_2^{(r)}\,i(t)\,\hat{I}_2 - \mu_1^{(r)}\,s(t)\,\hat{I}_1 +$$

$$+ \beta\,s(t)^2 + \gamma i(t)\,s(t) + \mu_1^{(r)}\,s(t)\,\hat{I}_1 - \mu_2^{(r)}\,i(t)\,\hat{I}_2 = 0.$$

The fact the total population size stays constant confirms that we are dealing with an
epidemic, i.e. it is an unusually large, short term outbreak of a disease as explained
in Sec. (2.2.1).

Chapter 6

Internship experience at Pharmacological Research Institute Mario Negri

6.1 The project

From November 2020 to March 2021, I had the opportunity to undertake an internship at the Pharmacological Research Institute Mario Negri, joining the *MUSE* (Mechanism Underlying the Selection and spread of carbapenem resistant Enterobacterales) project. Diffusion of multi drug resistant bacteria in critically ill patients during their stay in intensive care units (ICUs) is governed by the same probabilistic laws at the basis of the dynamics of outbreaks of infectious diseases such as the SARS-CoV-2 pandemic. Further details about this analogy are explained in this section.

6.1.1 MUSE - Mechanism Underlying the Selection and spread of Carbapenem-resistant Enterobacteria

In 2016 the project *MUSE* won the Finalized Research call with the Mario Negri Institute as Partner. The study aims to improve knowledge of the trend and epidemiological characteristics of colonization and infection sustained by carbapenem

resistant Enterobacterales (CREs). In particular, the objectives of this research are
the following.

- Description of the molecular epidemiology of CREs and the relative pathways
  of diffusion in 30 representative Italian ICUs (Intensive Care Units).

- Identifying and quantifying, through a multivariate statistical model, the role
  of the main factors in the selection and transmission of CREs, including the
  biological characteristics of the strain.

- Identify, through an *ad hoc* study based on qualitative observation, the 5 best
  and 5 worst ICUs in terms of control of the spread of CRE.

- Draw a Decalogue on what to avoid and what to improve to control the spread
  of CREs, and disseminate the document among the 477 Intensive Care Units
  that joined GiViTI (Italian Group for the evaluation of Intensive Care Units
  Interventions).

The study is aimed at the 158 Italian ICUs belonging to the GiViTI network
who have expressed interest in the increasingly widespread problem of infections.

6.1.2 Background

Enterobacterales are among the most common causes of infections associated with
health practices [55]. The emergence of CREs, mostly Klebsiella pneumoniae (Kp),
has become a major health problem worldwide. CREs in fact, are difficult to treat
and cause infections with high morbidity and mortality. Besides increasing the risk
of patient mortality, these infections also cause an increase of the costs associated
with health care. This burden is particularly high in intensive care units (ICUs),
where the rate of infections associated with healthcare practices is particularly high.
Italy, in particular, is one of the countries where CREs have become endemic, with
rates of Carbapenem-Resistant Klebsiella (CRKp) above 30% among Kp isolates
[56]. The clinical and epidemiological impact of CREs in Italian ICUs is confirmed
by data from the GiViTI network (Italian Group for the Evaluation of Interventions
in Intensive Care), composed by over 250 intensive care units located throughout

Italy and abroad [57].

CREs usually show a sensitivity profile towards very few antibiotics, such as colistin and tigecycline, and the extensive use of these molecules will over time lead to the selection of strains resistant to these molecules as well. At the same time, very few new drugs with activity against CREs are expected in the near future and, once in use, they will not be immune to antibiotic-resistance phenomena. In this scenario, all possible strategies must be put in place to try to control the spread of CREs, based on prevention of patient-to-patient spread and antibiotic stewardship programs. In particular the latter represents a way contribution in terms of appropriateness of antibiotic therapy to treat patients in a better way, to reduce side effects and bacterial resistance, and to contain costs. To this end, it is essential to understand and monitor the mechanisms of CRE diffusion in ICUs and of the complex interaction of the factors involved.

Data from the GiViTI network suggest, in fact, that different ICUs have different capacities to control the spread of CRE. This may be due to several variables, including patient characteristics, clinical practice, organizational and structural factors, as well as specific characteristics of CRE strains circulating in intensive care units. A better understanding of the complex interplay between these factors is fundamental to improve the strategies for the control of the diffusion of CRE in these facilities.

6.1.3 GiViTI group

The GiViTI (Italian Group for the Evaluation of Intensive Care Units Interventions) is a network of Italian and foreign ICUs that began its activity in 1991. The aim of the group is to promote and implement independent research projects, oriented to evaluation and to the improvement of the quality of care and a more rational use of resources. GiViTI currently involves 477 Italian and foreign ICUs.

The so-called *Margherita-PROSAFE* project aims at evaluating ICUs performance since 2002. All information are recorded on a special software and are accompanied by the respective definition, in order to ensure maximum comparability between the different intensive care units. In addition, an automatic review of the quality of the information collected is carried out in real time. Further the modular structure

of the software allows to easily integrate the basic data collection (the *core* of the daisy) with specific data collections for particular research projects (the *petals* of the daisy). In this way, the software becomes a tool that promotes both the efficiency and the quality of the department's research work.

6.1.4 Structure of the study

The study is observational, prospective, multicentre and non-profit. It is conducted in 30 Italian Intensive Therapies belonging to the GiViTI network that already use the Margherita-PROSAFE software for the collection of clinical data.

The study is divided into two phases:

1. The first phase of the study involves all the ICUs participating to the project and consists in the collection of the clinical, epidemiological and microbiological data of all hospitalized patients.

2. The second phase of the study consist in a preliminary analysis of aimed at evaluating each ICU based on its capability to limit the transmission of CREs from patient to patient: the 5 ICUs with the best performances and the 5 with the worst will be recruited for qualitative evaluation of their ability to control the spread of CREs.

The study will have a total duration of 36 months. Patient enrollment will last for a maximum of 15 months.

The study is aimed at the 158 ICUs joining the GiViTI network who have expressed interest in the increasingly widespread problem of infections. The 30 ICUs of the study will be selected starting from these 158 on the basis of the practices adopted in the ward with respect to the program of active colonization surveillance i.e. only ICUs who regularly carry out surveillance cultures for CREs will be recruited for the MUSE study.

Phase 1 of the study: Data Collection

The Margherita-PROSAFE software, currently in use in about 250 ICUs in 7 countries, will be used for data collection. This software consists of a *core*, whose com-

pilation is mandatory for all centers that use it, and a series of possible expansions
called *petals*, whose installation is optional. In the core of the Margherita-PROSAFE
program, the following data are collected.

- Main clinical-anamnestic data on admission: age, sex, origin, type, comorbidity, severity, reason for admission and diagnosis of entry);

- Data that describes the patient condition during the hospital stay: procedures, aids and their duration, pathologies and organ insufficiencies that have arisen;

- Data at discharge: outcome at ICU and hospital discharge.

In addition to the compilation of the core, the collection of data in two specific petals
is expected for the MUSE study. The first one, *Surveillance Infections Petal*, is dedicated to the surveillance of infections in the ICU and the collected data regards the
site of infection, kind of microrganism, date of onset, its origin for infections present
at admission or during stay (out-of-hospital, acquired in a ward hospital or acquired
in other ICU), the maximum severity reached (infection without sepsis, sepsis, septic
shock). The second Petal, called *MUSE Petal*, includes information about all CRE
infections: microrganism, locations, maximum severity reached, code of the isolated
microrganism. Only for the substudy on the 10 ICUs with best and worse performance antibiotic administered to the patient, data relating to the type of therapy,
the active ingredient, the start and end date of therapy, the dosage and the route
of administration will be collected using an electron health record (MargheritaTre),
developed by GiViTI [59].

The quality control of the collected data is carried out in real time during the compilation of the *petals* through multiple checks of the validity and congruence of the
data.

PROSAFE has a client-server architecture. All data of patients admitted to a single ICU are stored locally in a server installed inside the hospital network. Data
can be input from multiple clients in the same network. Pseudonymised data are
syncrhonized with a central server at Mario Negri Institute for Pharmacological
Research IRCCS where researchers cannot access patients' direct identifiers such
as name, surname, social security number, or birth date. In PROSAFE data are

stored in JSON format in a SQLite database. Once they are synchronized with the
central server, they are stored in a PostgreSQL database in a flat format (one row
per patient and variable). For the analysis, they are loaded in R obiects, where they
are managed though several tables in the form of one row per patients, for variables
that are measured once per patients (*e.g.*, age, comorbidities, clinical conditions
at admissions), or multiple rows per patients, for variables that can be measured
several times per patient (*e.g.*, treatment dates, bacteria responsible of infections,
etc. . .).

All the CRE samples isolated from colonized or infected patients will be collected
and stored by the microbiology laboratory of the participating ICUs. Those samples
will be transferred to the laboratory of the Microbiology and Virology Operating
Unit of Careggi University Hospital (FI), where they will be characterized for sus-
ceptibility to antimicrobial agents by MIC tests and subjected to whole genome
sequencing analysis (WGS) to extract information on: clonality and phylogeny, de-
terminants of antibiotic resistance (resistome), determinants of virulence (viruloma)
and plasmid content (plasmidome). These data will be associated, during the anal-
ysis, with the clincal data of each patient collected in the ICU with the PROSAFE
sofware.

Phase 2 of the study: Qualitative Analysis

Each of the ICUs selected for this phase will be monitored by an intensivist and a
nurse, trained to perform direct observations in the field and semi-structured inter-
views. The intensivist-nurse couples will be trained to perform direct observation
in the field and the semi-structured interview. In each ICU, the field observation
will focus on infection control practices, such as ICU structure, access to visitors,
organization of the work of nurses and doctors, hand and environment hygiene, man-
agement of colonized/infected patients, diagnosis of infection, antibiotic prophylaxis,
empiric/targeted antibiotic therapy.

6.1.5   Statistical analysis of the data

The statistical analysis will be conducted by the Laboratory of Clinical Data Science at the Mario Negri Institute for Pharmacological Research IRCCS in Ranica. The main analysis will focus on the first colonization/infection event that arose during the stay in ICU due to a CRE clone already present within the ward. The proportion will be used as a descriptive statistic for categorical and ordinal variables, the median and the inter-quartile interval for ordinal and continuous variables, the mean and standard deviation for continuous variables. The 95% confidence intervals will be calculated for each estimate of interest.

The observation time for each patient will begin at admission to ICU and will end upon discharge or death. Factors such as the occurrence of clinical procedures or antibiotic treatments during the observation period will be considered in a new model as time-dependent variables. If patients with multiple infections reach a sufficient number, ad hoc models (Cox models for repeated events) will be developed to identify the factors related to this type of event.

If the data collected will provide sufficient statistical power, any predictors of patient mortality, including microbial clones, will be evaluated.

6.2   Experimental study

During the internship at the Pharmacological Research Institute Mario Negri, I applied computer science and mathematical tools I learnt during master degree and the internship itself in order to describe the transmission of Carbapenem resistant Microrganisms in intensive care units.

During the internship I worked for the following objectives:

- Comprehension of the functioning and implementation of Margherita-PROSAFE software;

- Understanding the functioning of data collection;

- Data management and data analysis;

- Management of missing data;

- Development of a mathematical model for the description of the diffusion of CRE in intensive care units;

- Estimation of the contact rate β and its confidence interval, through Monte Carlo Methods. This parameter is in strict correlation with the contact rate defined in Sec. (2.2.1) that is the average number of adequate contact of a person for unit time that allows the transmission of CRE inside ICU. Here we will address to it as *transmission parameter*;

- Graphic visualization of the data in order to allow a better understanding of the spread of the colonization inside ICUs.

The first task I needed to carry out in order to work on this project was to understand how Margherita-PROSAFE works and get the hang of it. According to which data were selected, distinct *petals* opens and different combination of missing or sloppy collected data could arise. The most relevant problem that occurred while analyzing the data was in fact that the compilation of the medical records could be non consistent or not complete and consequently it became important to understand how to take into consideration these patients since they could be both unrecognized carriers of the CRE or infection-free individual. Depending on their being *cre* or *non − cre* they would contribute in rising or decreasing β, the transmission parameter that we need to estimate in order to evaluate the capability of an ICU to contain the spread of these microrganism.

Thank to this thesis I had direct access to R objects constructed from original PROSAFE data, as described in Sec. (6.1.4). All the analysis were performed using R software Version 1.3.1093. The following step was indeed to identify which variable broadcast to R were the corresponding on PROSAFE software in order to start elaborating the data.

We implemented three main R codes:

(*) The first code allows to classify every patient day by day in one of the categories, *cre*, *non − cre* or *unknown*, according to his health status.

(**) The second one allows to determine how the contagion is transmitted inside every ICU and answers the following question: *how many colonization/infections due to transmission are there? How many colonization/infections without transmission are there? How many colonization/infections at admission are there?*

Further a graphical visualization of the spread of contagion is proposed.

(***) The third code allows to estimate the confidence interval of β, the transmission parameter trough the Monte Carlo method **??** and present its confidence interval.

6.2.1 Classification of patient

The first code we implemented in R language allowed to categorize each patient into *cre, non-cre, unknown* according to their medical records. The scenario throughout which people could determine their status are colonization, i.e. when a germ is present in a person and can grow without showing symptoms or cell damage, or infection.

There are two different moments during which the presence of a germ can be detected, that are:

- at admission, which means that the germ is carried from outside the ICU, thus infection occurred without transmission between individuals staying in the ICU, but a new carrier of the infection arise, who represents a possible way to spread the infection;

- during patient's stay in the ICU, which means that either this patient has been infected by another individual inside the ICU either that he could already be colonized/infected. This case could be due to poorly collected data or erroneously analyzed exams, for example, the patient has not been checked, either the exam has not showed the presence of the germ despite it was there. Thus this was a previously ***unknown*** individual that turns out to be a ***cre***.

In this project we considered the following species of Enterobacterales: *Klebsiella, Escherichia Coli, Enterobacter, Citrobacter, Proteus* and *Serratia* (*List 1). They

can be weather sensible or resistant to carbapenem. Tests for CRE colonization are performed through a rectal swab and directly search only for CRE. The presence of carbapenem susceptible Enterobacteria or other microorganisms is not revealed. If the microbiological test is consequent to the onset of an infection, the biological sample is first analysed to assess the presence of any microrganism. Resistance to antibiotic molecules, including carbapenems, is tested for each isolated bacterium.

Since *Margherita-PROSAFE* has been planned to collect data for several studies, there are two particular infections, from which a CRE germ could be detected, that must be treated separately because their data structure is different from other infections. They are primary bacteriemia and pneumonia. Further their occurrences are reported separately based on the fact the CRE was present only during the first infective episode, only in the following the first episodes or it was present both during the first and the following episodes. Since this division is not relevant for our study we merged conveniently the cases into: first episode or following episodes.

We need to introduce some conditions, which their logical values, i.e. if they are true or false, will be then exploited in order to classify every person day by day in *cre, non-cre* or *unknown*.

Cre patient

- Rectal swab for CRE colonization surveillance is collected at admission and it results positive;

- Rectal swab for CRE colonization surveillance is collected during stay and it results positive;

- The patient has an infection at ICU admission and the sample presents a microrganism among *List 1* which has been tested to be resistant to carbapenems;

- The patient has an infection during stay and the sample presents a microrganism among *List 1* which has been tested to be resistant to carbapenems.

- If the patient has primary bacteriemia or pneumonia, weather in the first or the following episodes, and the test presents a CRE microorganism among *List 1*.

Non-cre patient

- Rectal swab for CRE colonization surveillance is collected at admission and it results negative;

- Rectal swab for CRE colonization surveillance is collected during stay and it results negative;

- The patient has no infection neither at admission nor during stay;

- The patient enters the ICU with an infection. The responsible microrganism is known and either it is not in *List 1* or it is in *List 1* but it is sensible to carbepenem;

- The patient is subjected to infection during stay. The responsible microrganism is known and either it is not in *List 1* or it is in *List 1* but it is sensible to carbepenem.

- If the patient has primary bacteriemia or pneumonia, weather in the first or the following episodes, but the test does not present carbapenem resistant microorganisms.

It is important to remember that in order to be categorised as a *non-cre* individual, none of the "*cre* conditions" should verify otherwise the patient is a CRE colonized/infected one.

Unknown patient

- Rectal swab for CRE colonization surveillance is not collected at admission;

- Rectal swab for CRE colonization surveillance is not collected during stay;

- The patient has an infection in admission but either no microrganism has been isolated or the microrganism isolated is from *List 1* but resistance has not been tested;

- The patient has an infection during stay but either no microrganism has been isolated or the microrganism isolated is from *List 1* but resistance has not been tested.

- If the patient has primary bacteriemia or pneumonia, weather in the first or the following episodes, and the test does not isolate any microorganism.

A patient is defined as *unknown* whether he had not all the necessary medical tests to establish if he is free or carrier of CRE, whether if he has an infection but the responsible microrganism is not known we can not say weather the infection is due to a CRE microrganism or not.

The code implemented makes a daily partition between the possibilities *cre*, *non-cre* and *unknown* i.e. a patient could be categorized into just one of the classes. This procedure is done for every single event during which an individual could become colonized/infected that are: colonization-admission x_1, colonization-stay x_2, infection-admission x_3, infection-stay x_4, bacteriemia/pneumonia - first episode x_5 and bacteriemia / pneumonia - following episodes x_5. A three-valued logical variable is assigned to each class i.e.

cre condition	TRUE
non-cre condition	FALSE
unknown condition	NA

Table 6.1: Assignment of the logical value to the "cre conditions".

This leads to the following logical implementation:

$$\textit{Final evaluation of the patient} \;=\; x_1 \,|\, x_2 \,|\, x_3 \,|\, x_4 \,|\, x_5 \,|\, x_6$$

Logical operations are defined in the algebra of three-values logical variables [61]. It means that it is sufficient to present a positive "*cre* condition" to be a *cre*, while

if different combination of only "*non-cre* and *unknown* conditions" are present the final result will be *unknown.*

Finally, taking into consideration the dates of each event and the relative status it is possible to classify day by day every single patient.

6.2.2 Estimate of transmission rate in Intensive Care Units

Once I had identified the "CRE-status" of each patient day by day, the following step was to investigate how the infection is transmitted in the ICU. Consider now the case of carbapenem-resistant germ Klebsiella Pneumoniae (KPC).

MUSE data collection started in May 2019 and, due to delays associated with the pandemic outbreaks of coronavirus is still ongoing. Futhermore, GiViTI closes data collection for patients admitted to ICU during one year in the month of March of the next year. For these reasons we analyzed data relative to patients admitted to ICU from May to December 2019.

For privacy issue I will call the three considered hospital *Centre A*, *Centre B* and *Centre C.*

The following graph (6.1), (6.2) and (6.3) show the following information:

- The black line shows the number of patients present in the ward from May to December of the year 2019.

- The red line shows the number of colonized and/or infected patients present in the ward, which represents our *cre* patients;.

- The orange line shows the number of non-colonized and non-infected patients present in the ward, which represents our *non-cre* patients;

- The light green line shows the number of *unknown* patients present in the ward, of which we are not able to say whether they are colonized/infected or not.

• The green dots indicate the days in which a colonized and/or infected with KPC patient was admitted to the ward (the size of the dot increases if 2 or more colonized and/or infected patients were admitted on the same day);

- The red dots indicate the days in which an already recovered patient turns out to be colonized and/or infected with KPC (also in this case the size of the dot is proportional to the number of colonized and/or infected patients). On these days, one or more patients colonized and/or infected with KPC are already present in the ward and it is possible to assume that the new cases are the results of transmission.

  It should be noted that each patient can give rise to only one red dot, namely a patient who first becomes colonized by KPC and then becomes infected, will be represented in the graph with a single red dot, on the day he became positive for colonization.

- The blue dots indicate the days in which cases of colonization and/or infection by KPC were detected during hospitalization without already colonized and/or infected patients being present in the ward. In this way, cases of colonization and/or infection probably not due to transmission are highlighted.

For each center a transmission coefficient β could be estimated. It describes the entity of the contagion due to transmission inside every ICU, though it evaluates the capacity to contain the infectious spread. The higher it is, the more the transmissions are, the worst it is. The lower it is, the less the contagion are, the better it is. According to this definition, as the coefficient increases, the risk in the single center of transmitting KPC from one patient to another increases. The coefficient is calculated for a period of 1000 days through the following formula:

$$\beta = 1000 \; \frac{C}{\displaystyle\sum_{d} L_d \, P_d} \tag{6.1}$$

where d indicates the days, C the number of colonized and/or infected patients during hospitalization due to probable transmission (red dots), L_d the patients "free" of KPC and P_d the number of patients "carriers" on that day.

β corresponds to the ratio between the colonized patient with respect to the patients at risk, i.e. the sum, day by day, of the number of susceptible to KPC patients multiplied by the number of colonized/infected patients on that day. Thus it is the ratio

between occurred contagions and all possible contagions.

The transmission parameter β answers the question: *How many transmissions of KPC occur per 1000 days of ICU stay?*
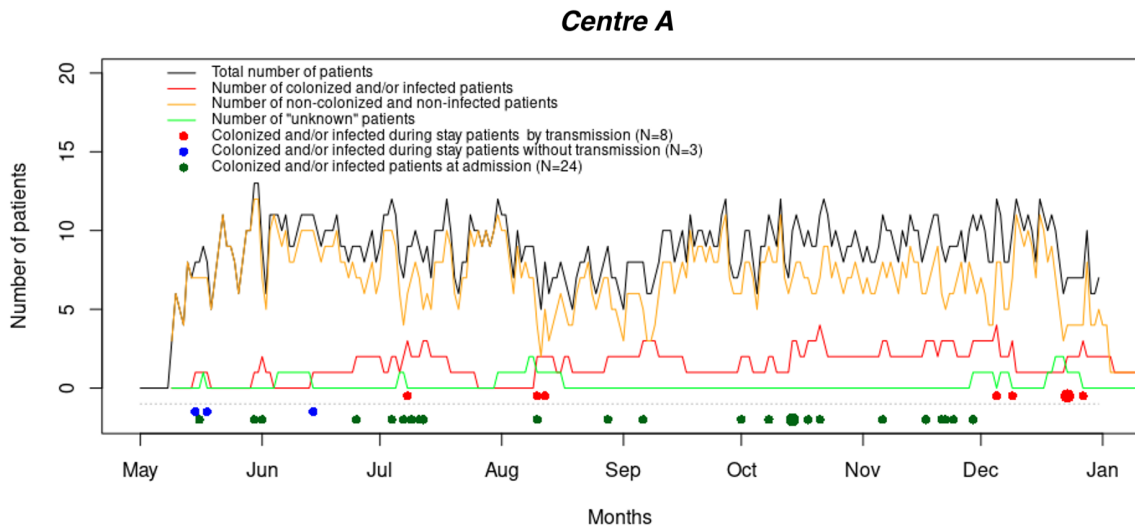
Figure 6.1: Transmission of Klebsiella among patients in ICU of *Centre A* (2019)

Center A sees an average of 9-10 patients hospitalized per day. Its way to control the infection spread is neither completely effective neither dramatic: the transmission coefficient β is equal to 1.46. *Center A* sees 24 colonized patients in admission and 11 cases that arose in hospitalization, of which 3 could not be attributable to transmission.

What is important to observe is that when a blue dot is present, that is when a colonization/infection occurs without any colonized/infected patient in the ward, we can see that a previously *unknown* individual is there in the ICU. After the blue dot appearance we have an increase of one in the number of *cre* individuals (red line), while we have a decrease of one in the number of the *unknown* individuals (light green line). This means that a patient was already colonized/infected when he entered the ward but he had not been detected.
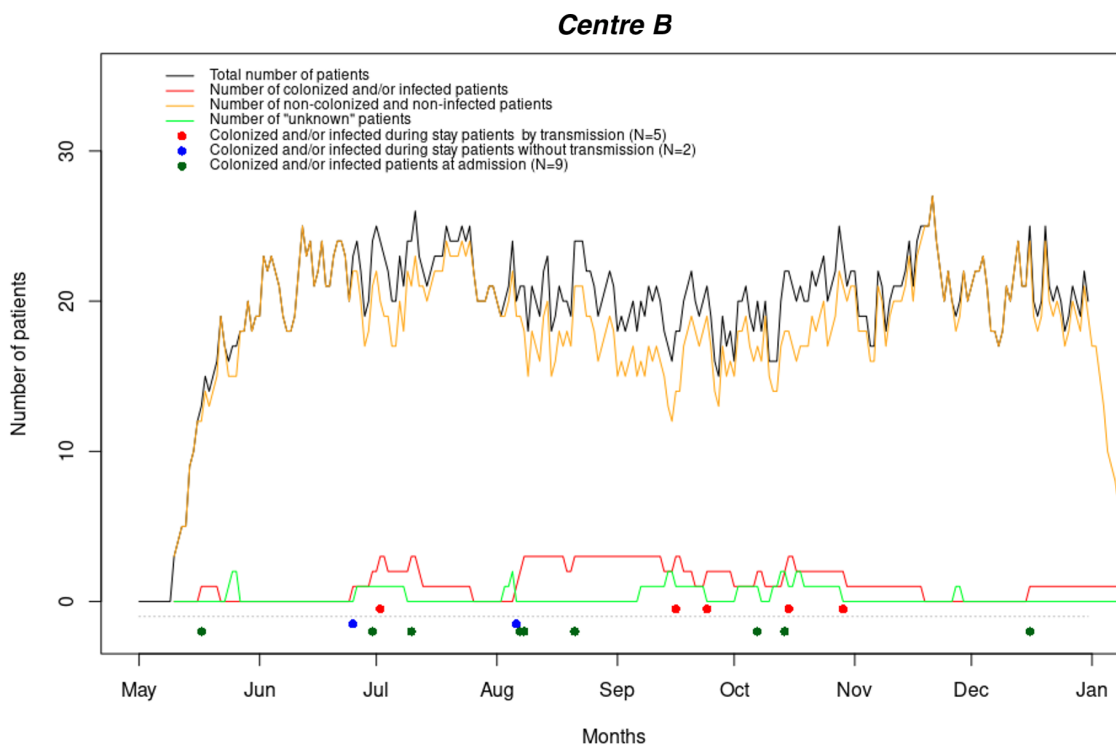
Figure 6.2: Transmission of Klebsiella among patients in ICU of *Centre B* (2019)

In *Center B* the average of patients hospitalized per day is 21. It results really efficient in controlling the infection spread: β is equal to 0.96. Despite the high number of patients present in the ward, the 9 cases of colonized/infected patients that are admitted do not cause an outburst of contagion and the transmission parameters is kept very low. The colonizations/infections due to transmission are 5, while the ones with no transmission are 2, for a total of 7 new infections during stay.

Center C has an average of 12 patients hospitalized per day. This centre has not suitable health protocols. It is shown by the transmission parameter, that is much higher than the coefficients of the other hospitals: β is equal to 3.19. With a total of 20 colonized/infected patients in admission this ICU has 12 new cases due to transmission and none without transmission. Anyway the absence of people that are colonized/infected without any other colonized/infected patient in the ward (blue dots) is a positive objective. It could be due a good surveillance test routine, that by the end results to be better than what we have observed in the other centres

with small transmission parameter. Though problem should lie in the poorly health practice.
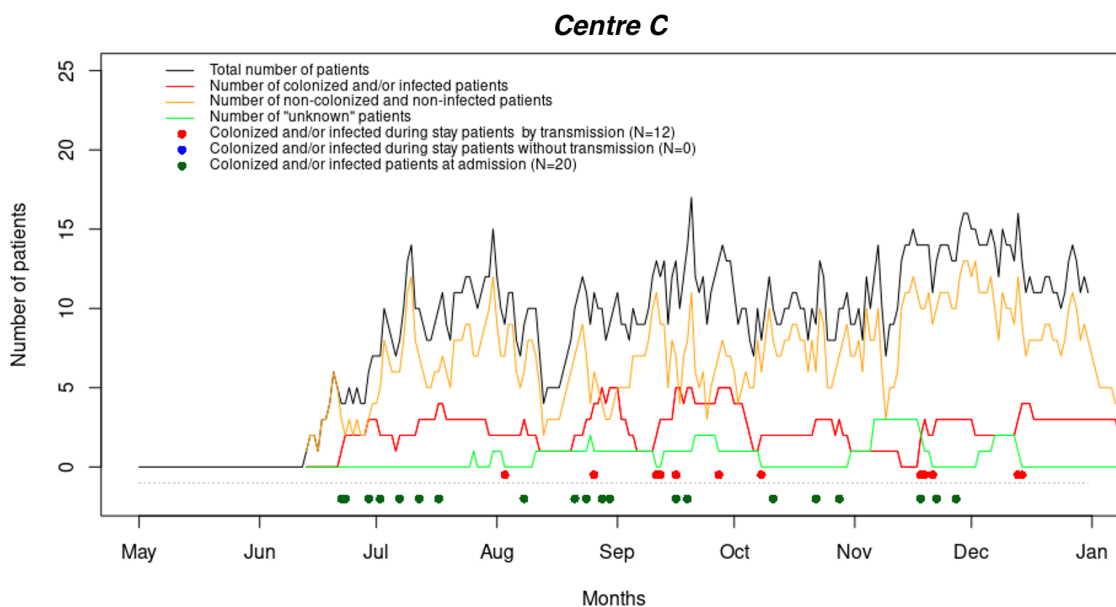
Figure 6.3: Transmission of Klebsiella among patients in ICU of *Centre C* (2019)

6.2.3 Monte Carlo simulation

The transmission coefficient β is estimated for the three Intensive Care Units taken into consideration in Sec. (6.2.2), *Centre A*, *Centre B* and *Centre C*, according to the data collected. In order to estimate the confidence interval of the parameter and the relative boxplot, which marks its first and third quartile, we performed a Monte Carlo simulation.

The Monte Carlo Methods (MCM) [62] replaces complex analytical procedures by computer intensive empirical analysis. It has been shown [63] to be an effective technique in situations where it is necessary to determine the sampling distribution of usually complex statistic with an unknown probability distribution using the data in a single sample.

The basic idea of Monte Carlo method is to simulate a complex physical process (e.g. the spread of an infectious disease in the intensive care units) made by several

events which can be represented by simple correlated stochastic variables with known distributions (e.g. the probability a susceptible individual becomes infected when he/she meets an infected individual). For a single realization i of this process, one can compute the estimator $\hat{\beta}_i$ of the investigated parameter β, the transmission rate. By repeating this procedure k times, one can construct the "MCM distribution" of the parameter β, and determine its mean, its standard error, or its confidence interval.

Note that Monte Carlo Methods are free of parametric assumptions common in traditional statistical techniques. The only assumption underlying this method is that the sample is representative of the population, a basic assumption which underlies any statistical technique. Monte Carlo Methods are most effective in cases where the sampling distribution of the statistic is so complex that it cannot be analytically derived and/or where the sampling distribution can be derived only under strict parametric assumptions and cannot be generalized when these assumptions are not satisfied. Without making any parametric assumptions, Monte Carlo method provides thus a way to construct the distribution function for the investigated parameter.

In our case, to simulate the evolution of contagion of intensive care units, we set the following data:

- β the transmission parameter, which is evaluated through formula (6.1);

- $f_{colonized}$ which represents the fraction of colonized patients in the ward.

These parameters are calculated according to the data of the relative centre. Once we assume the values of these parameters we can simulate the phenomena of transmission and evaluate the distribution function for the investigated parameter.

The physical process of transmission can be modeled by a complex stochastic process made by n random dichotomous variables $X_1, X_2, ..., X_n$, each one representing the state of colonization of a single patient for each day of his/her permanence in ICU. The estimator of the transmission coefficient β is a function of the set $\{X_i\}_{i=1,...,n}$ (see Eq. (6.1)). The stochastic variable X_i are strongly correlated, since the probability that a susceptible patient become colonized on a certain day of

permanence in ICU depends on how many colonized or infected patients are present
in ICU on the same day, which in turn is correlated to the number of infected present
the previous days and so on. Thus, the analytical computation of the distribution
of X_i is not straightforward.

However, a realization of this stochastic process is easily obtained through a Monte
Carlo simulation, through the following procedure

1. Simulate the evolution of the infection inside the intensive care unit during a
   year, *i.e.* we construct a realization of each X_i, by sampling from two binomial
   distributions, with mean equal to either p_1 or p_2 where:

   - p_1 represents the probability that a new patient admitted to the ward is
     colonized/infected and assumed to be equal to $f_{colonized}$ for each patient;

   - p_2 represents the probability that a patient becomes colonized/infected
     in the ward p_2 is proportional to the number of infected people present in
     the ward that day, where the proportionality constant is the transmission
     coefficient.

2. Compute $\tilde{\beta}$: the value of β obtained by using the MCM sample;

3. Repeat k times steps 1 and 2. For standard error estimation, k is recommended
   to be at least 100 (for more details see Chapter 7 of [65]). We chose $k =
   1000$ and by replicating k times steps 1 and 2, we obtain a Monte Carlo
   approximation of the distribution of β.

According to the collected data for *Centre A*:

- $\beta = 3.20$;

- $f_{colonized} = 0.02$.

The 95% confidence interval is: $I_c = (0.63, 5.90)$. At first glance the confidence inter-
val seems to be extremely large. In fact, the transmission coefficient β is relatively
small, so that the appearance of new colonizations/infections during ICU stay is
unlikely. Thus, the number of colonized patient during the whole year is small, and,
accordingly, variability is large.
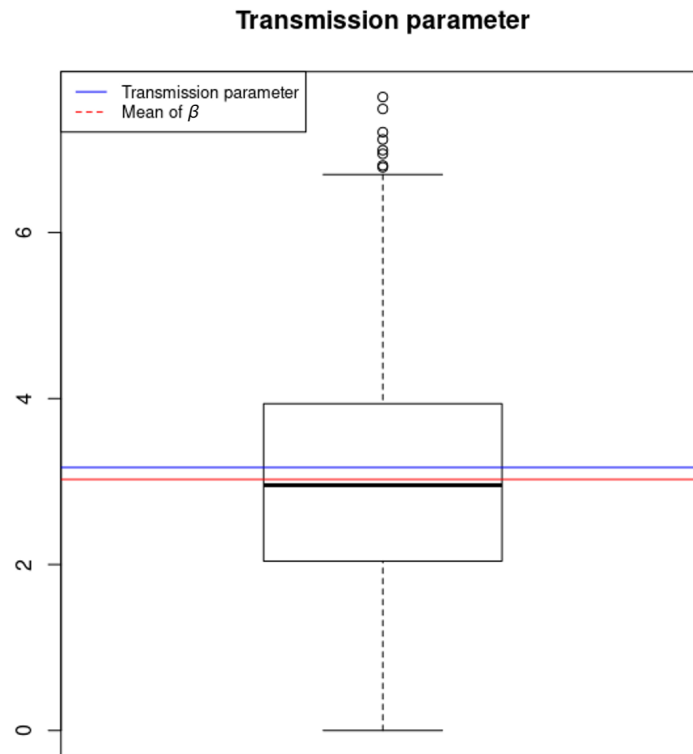
Figure 6.4: Example of estimation of β of *Centre A* trough Monte Carlo method.

Furthermore we can observe that the mean (red line) almost coincide with the median (bold black line), while it slightly differs from the value of the transmission parameter the simulation was based on. This suggests that there is a small bias in the estimator $\hat{\beta}$ obtained through Monte Carlo algorithm. However, this bias is much smaller than the confidence interval and it does not significantly affect the results.

For the second centre, *Centre B*, the collected data shows:

- $\beta = 0.96$;

- $f_{colonized} = 0.02$.

The 95% confidence interval is: $I_c = (0.30, 1.58)$. In Figure (6.5) we can observe that as the number of new colonizations/infections decreases the length of confidence interval tightens. As before a small bias due to Monte Carlo simulation arises from the difference between the transmission parameter β evaluated trough real data and
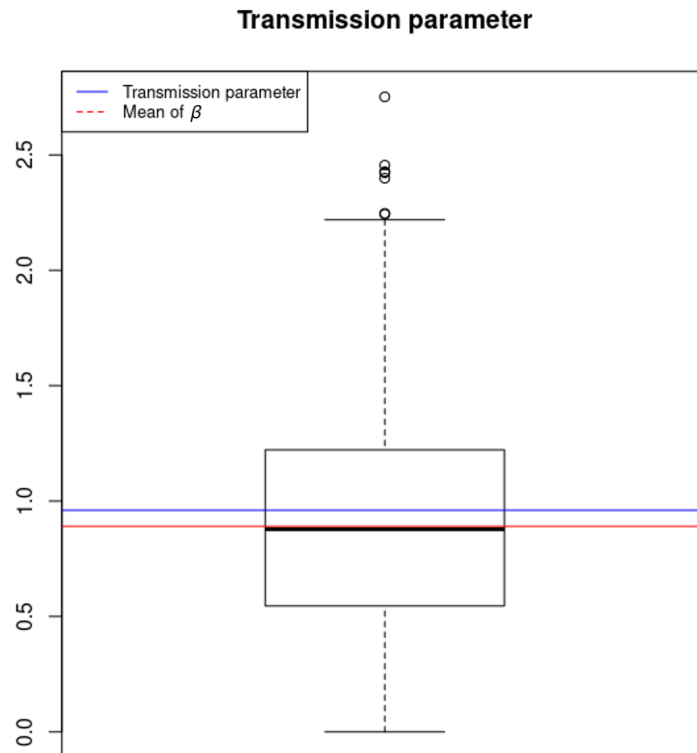
Figure 6.5: Example of estimation of β of *Centre B* trough Monte Carlo method.

the mean of this parameter estimated with MCM.

Finally, for *Centre C*, we have:

- $\beta = 3.19$;

- $f_{colonized} = 0.08$.

The 95% confidence interval is: $I_c = (1.58, 4.54)$.

Centre C shows a similar situation to the first case of *Centre A* (see figure 6.4).
Compared to this case we note that the length of the interval, although it remains
wide, decreases. This is due to a higher fraction of colonized at admission patients.
As for *Centre A* and *Centre B* a small bias due to Monte Carlo simulation arises.
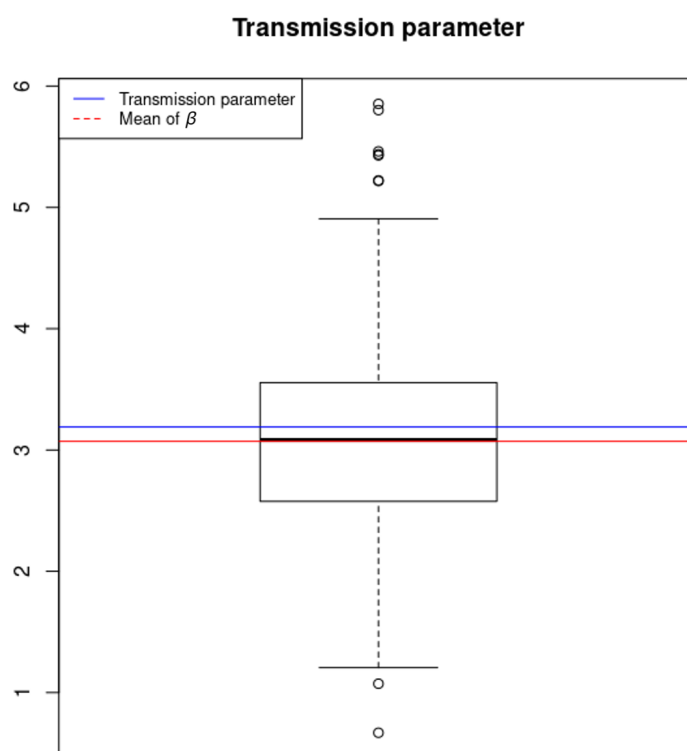
Figure 6.6: Example of estimation of β of *Centre C* trough Monte Carlo method.

Chapter 7

Conclusion

The aim of this thesis is derive a rigorous mathematical model from the kinetic theory of gases in order to describe the large-scale spread of the SARS-COV-2 epidemic. Since people have less predictable behavior than gas molecules, the proposed representation is way more complex. The main feature of the model is the use of an "interaction potential", as for the gas molecules, to describe the spread of the infection which can thus occur not only by direct contact between two individuals, but also at a distance. The interactions within each population and the action of the immune system have been modeled by means of a stochastic description to highlight the random aspects related to the onset and progression of the coronavirus disease. The transition between different populations has been described in analogy with the laws governing reactive gas mixtures. The model has been defined at the microscopic scale and the, through an average procedure, the corresponding macroscopic equations, for the evolution of the size of the different populations, have been derived. This approach allowed us to match our model with different compartmental epidemiological models existing in the literature. As a future research, it would be interesting to examine, for example, the effect of quarantine and the effect of vaccines on the evolution of the epidemic. Great hopes are in fact placed in the vaccine but also in other approaches which are not only able to stimulate / regulate the immune system in an optimal way, but they are also able to inhibit viral replication, thus preventing the progression of the disease. In this perspective, it is clear that only a multidisciplinary approach can provide various solutions for the description

and future prophylaxis of the infection.

The fact that the laws underlying the spread of an infectious disease are the same as those underlying the spread of Carbapenem-resistant Enterobacterales (CRE) has also made it possible to draw a parallel between CRE and SARS-CoV-2. This study, called MUSE (Mechanism Underlying the Selection and spread of carbapenem resistant Enterobacterales), was carried out in collaboration with the Mario Negri Research Institute and allowed an experimental comparison with the theoretical study. Carbapenem-Resistant Enterobacterales make the hosts completely immune to the use of the carbapenem antibiotics, so that pharmacological treatments and consequently recovery become way more difficult. This is why it is so important to stop its spread. Thanks to the use of special software (Margherita-PROSAFE) and R it was possible to carry out a work of data collection and analysis in order to estimate the transmission coefficient. Furthermore, thanks to the use of the Monte Carlo method it was possible to evaluate the distribution function for the investigated parameter. Through the simulation of the complex spread in hospital we were able to propose a confidence interval for the value of the transmission rate. Thanks to this method all the statistics useful for further studies can be obtained. One of the greatest difficulties we met was certainly the presence of incomplete or missing data, caused by hasty or sloppy compilation of clinical records. The problem of incorrect or missing data can result in an inaccurate transmission parameter, since an individual can be both a carrier or disease free. The results obtained are satisfactory, but the study is not yet concluded and the Mario Negri Research Institute is going on completing and improving the outcomes. This study can reveal useful both for the description and control of Covid-19 spread (or of a new occurring epidemic), and to contain and reduce the transmission of infections inside the intensive care units.

Appendix A

Liapunov - LaSalle invariance principle

Theorem A.0.1 (Liapunov - LaSalle invariance principle).

Let $\Omega \subset D$ be a compact set and a positively invariant for the system

$$\dot{x}(t) = f(t) \tag{A.1}$$

Let $V : D \to \mathbb{R}$ be a smooth and derivable function with negative semidefinite derivative i.e. $\dot{V}(x) \leq 0$ in Ω, $E \subset D$ be the set of points such that $\dot{V}(x) = 0$ and $M \subset E$ be the largest invariant contained in E.

Then every solution of the system starting in Ω tends to M for $t \to \infty$.

Proof. Let $x(t)$ be a solution starting in Ω. Then $V(x(t))$ admits a limit for $t \to \infty$.
Moreover let L^+ be the set of positive limit point, so $L^+ \subset \Omega$ as Ω is closed.
By definition of L^+, for all $p \in L^+$ there exists a sequence $\{t_n\}$ that $t_n \to \infty$ as $n \to \infty$ such that $x(t_n) \to p$ as $n \to \infty$.
By continuity of $V(x)$ we have that $V(p) = \lim_{n \to \infty} V(x(t_n)) = a$. Then $V(x) = a$ in L^+ and since L^+ is invariant $\dot{V}(x) = 0$ in L^+.
Therefore $L^+ \subset M \subset E \subset \Omega$ and since $x(t) \to p \in L^+$ we also have that $x(t) \to p \in M$. $\qquad \square$

Appendix B

Routh-Hurwitz criterion

Theorem B.0.1 (Routh-Hurwitz [66]). *Consider an nth-order polynomial in s:*

$$p(s) = a_0 + a_1 s + a_2 s^2 + \dots + a_{n-1} s^{n-1} + a_n s^n, \tag{B.1}$$

where $a_i \in \mathbb{R}$, $i = O, 1, \dots, n$ and $a_n > 0$ and $a_0 \neq 0$.

Suppose none of the divisors are zero and construct the Routh table i.e.

$$R(p) = \begin{bmatrix} a_n & a_{n-2} & a_{n-4} & a_{n-6} & \dots \\ a_{n-1} & a_{n-3} & a_{n-5} & \dots \\ b_{n-1} & b_{n-2} & \dots \\ c_{n-2} & c_{n-3} \end{bmatrix}$$

using the notation:

$$b_{n-2} = a_{n-2} - \frac{a_n}{a_{n-1}} a_{n-3} \qquad b_{n-4} = a_{n-4} - \frac{a_n}{a_{n-1}} a_{n-5} \qquad \dots \tag{B.2}$$

$$c_{n-4} = a_{n-3} - \frac{a_{n-1}}{b_{n-2}} n_{n-4} \qquad c_{n-6} = a_{n-5} - \frac{a_{n-1}}{b_{n-2}} n_{n-6} \qquad \dots \tag{B.3}$$

$$\dots \tag{B.4}$$

ie. in general

$$k_{i,j} = \frac{\begin{vmatrix} k_{i-2,1} & k_{i-2,j+1} \\ k_{i-1,1} & k_{i-2,j+1} \end{vmatrix}}{-k_{i-1,1}}$$

Then $p(s)$ is Hurwitz (i.e., $p(s)$ has all its zeros in the open left half-plane) if and only if each element of the first column is positive, i.e., $a_n > 0, a_{n-1} > 0, b_{n-2} > 0, \dots$

Bibliography

[1] C.I. Siettos, L. Russo, *Virulence 4*. 295-306, 2013.

[2] W.O. Kermack, A.G. McKendrick, *Proceedings of the Royal Society A 115*. 700-721, 1927.

[3] C. Cercignani, R. Illner, M. Pulvirenti, *The mathematical theory of dilute gases*. Springer. 1994.

[4] N. Bellomo, *Modeling complex living systems*. Birkhaeuser, 2008.

[5] Gruppo di Lavoro ISS Immunologia COVID-19 *Strategie immunologiche ad interim per la terapia e prevenzione della COVID-19*. Versione del 4 giugno 2020.

[6] M. Bisi, S. Lorenzani,*Physics of Fluids 28*, pp. 052003-052003-21, 2016.

[7] S. Lorenzani, *Physics of Fluids 31*, pp. 072001-072001-17, 2019.

[8] G. Bertolini, C. Rossi, D. Crespi, S. Finazzi, et al., *Intensive Care Medicine 37*. 1746-1755, 2011.

[9] N. T. J. Bailey, *The Mathematical Theory of Infectious Diseases*. Hafner, New York, second ed., 1975.

[10] W.O. Kermack, A.G. Mckendrick:*Contributions to the mathematical theory of epidemics*. Proc. Roy. Soc. (A115). 700-721, 1927.

[11] R. M. Anderson and R. M. May, *Population Biology of Infectious Diseases*. Springer-Verlag, Berlin, Heidelberg, New York, 157, 1982.

[12] *Infectious Diseases of Humans: Dynamics and Control.* Oxford University Press, Oxford. 306, 1991.

[13] H. W. Hethcote, H. W. Stech, and P. van den Driessche, *Periodicity and stability in epidemic models: A survey, in Differential Equations and Applications in Ecology, Epidemics and Population Problems.* S. N. Busenberg and K. L. Cooke, eds., Academic Press, New York. 65–82, 1981

[14] H. W. Hethcote, *The basic epidemiology models: models expressions for R_0, parameter estimations and applications.* Mathematical understanding of infectious disease dynamics: 1-62.

[15] Z. Feng, H.R. Thieme, *Endemic models with arbitrarily distributed periods of infection I: general theory.* SIAM. J. Appi. Math. 803, 2003.

[16] L-I, Wu, Z. Feng, *Homoclinic bifurcation in an SIQR model for Childhood disease.* J. Diff. Equ. 150-167, 2000.

[17] Zhien Ma, *Some Recent Results on Epidemic Dynamics Obtained by Our Group.*

[18] Stefan Ma, Yingcun Xia, *Modeling and dynamics of infectious diseases.* 1-35, 2009.

[19] J.Q. Li, Z.E. Ma, *Stability analysis for SIS epidemic models with vaccination and constant population size. Discrete and Continuous Dynamical Systems Series B.* 635-642, 2004.

[20] H. Hethcote, Z.E. Ma, S. Liao, *Effects of quarantine in six endemic models for infectious disease.* Math. Biosci. 141-160, 2002.

[21] J.Q. Li, Z.E. Ma, Y.C. Zhou, *Global analysis of SIS epidemic model with a simple vaccination and multiple endemic equilibria.* Acta. Math. Sci. 83-93, 2006.

[22] Gruppo di Lavoro ISS Immunologia COVID-19, *Strategie immunologiche ad interim per la terapia e prevenzione della COVID-19.* Rapporto ISS COVID-19, 04 giugno 2020.

[23] ProMED, *Undiagnosed pneumonia - China (HU): RFI.* ProMED-mail 2020. https://promedmail.org/promedpost/?id=20191230.6864153.

[24] Tyrrell DA, Bynoe ML, *Cultivation of viruses from a high proportion of patients with colds.* Lancet. 1(7428):76-77, 1966.

[25] *GISAID Global Initiative on Sharing All Influenza Data. Phylogeny of SARS-like betacoronaviruses including novel coronavirus (nCoV).*

[26] Zhou P, Yang XL, Wang XG et al., *A pneumonia outbreak associated with a new coronavirus of probable bat origin.* Nature 2020.

[27] Zhou P, Yang X-L, Wang X-G, Hu B, Zhang L, Zhang W, Si H-R, Zhu Y, Li Huang C-L, Chen H-D, Chen J, Luo Y, Guo H, Jiang R-D, Liu M-Q, Chen Y, Shen X-R, Wang X, Zheng X-S, Zhao K, Chen Q-J, Deng F, Liu L-L, Yan B, Zhan F-X, Wang Y-Y, Xiao G, Shi Z-L., *Discovery of a novel coronavirus associated with the recent pneumonia outbreak in humans and its potential bat origin.* 2020.

[28] Rottier PJM., *The coronavirus membrane glycoprotein.* Siddell SG (Ed.). The Coronaviridae. Boston, MA: Springer. 115-137, 1995.

[29] Adhikari SP, Meng S, Wu YJ, et al. *Epidemiology, causes, clinical manifestation and diagnosis, prevention and control of coronavirus disease (COVID-19) during the early outbreak period: a scoping review.* Infect Dis Poverty. 9-29, 2020.

[30] Lauer SA, Grantz KH, Bi Q, et al., *The Incubation Period of Coronavirus Disease 2019 (COVID-19) From Publicly Reported Confirmed Cases: Estimation and Application.* 577-582, 2020.

[31] Zhang Y, Chen C, Zhu S, Shu C, Wang D, Song J, Song Y, Zhen W, Zijian F, Wu G, Xu J, Xu W. *Isolation of 2019-nCoV from a stool specimen of a laboratory-confirmed case of the coronavirus disease 2019 (COVID19).* China CDC Wkly 2(8): 172(9), 123–124, 2020.

[32] Chen H, Guo J, Wang C, et al., *Clinical characteristics and intrauterine vertical transmission potential of COVID- 19 infection in nine pregnant women: a retrospective review of medical records.* 2020.

[33] Chen N, Zhou M, Dong X, et al., *Epidemiological and clinical characteristics of 99 cases of 2019 novel coronavirus pneumonia in Wuhan, China: a descriptive study.* 395(10223), 507-513, 2020.

[34] Magro C, Mulvey JJ, Berlin D, et al., *Complement associated microvascular injury and thrombosis in the pathogenesis of severe COVID-19 infection: a report of five cases.* S1931-5244(20) 30070-0, 2020.

[35] Wang D, Hu B, Hu C, et al., *Clinical Characteristics of 138 Hospitalized Patients With 2019 Novel Coronavirus- Infected Pneumonia in Wuhan.* China. JAMA. 323(11): 1061-1069, 2020.

[36] Sallard E, Lescure FX, Yazdanpanah Y, Mentre F, Peiffer-Smadja N., *Type 1 interferons as a potential treatment against COVID-19.* Antiviral Res. 178:104791, 2020.

[37] Mantlo E, Bukreyeva N, Maruyama J, Paessler S, Huang C., *Antiviral activities of type I interferons to SARS- CoV-2 infection .* Antiviral Res. 179:104811, 2020.

[38] Maggi E, Canonica GW, Moretta L., *COVID-19: unanswered questions on immune response and pathogenesis.* J Allergy Clin Immunol. S0091-6749(20)30631-X, 2020.

[39] Matricardi PM, Dal Negro RW, Nisini R. *The first, holistic immunological model of COVID-19: implications for prevention, diagnosis, and public health measures.* Pediatr Allergy Immunol. 2020.

[40] Gao T, Hu M, Zhang X, et al. *Highly pathogenic coronavirus N protein aggravates lung injury by MASP-2- mediated complement over-activation.* medRxiv preprint. 2020.

[41] Jansen JM, Gerlach T, Elbahesh H, Rimmelzwaan GF, Saletti G. *Influenza virus-specific CD4+ and CD8+ T cell-mediated immunity induced by infection and vaccination.* J Clin Virol. 44-52, 2019.

[42] Gruppo di Lavoro ISS Ambiente e Rifiuti*Indicazioni ad interim sulla gestione e smaltimento di mascherine e guanti monouso provenienti da utilizzo domestico e non domestico.* Versione del 18 maggio 2020. Roma: Istituto Superiore di Sanità; 2020. (Rapporto ISS COVID-19 n. 26/2020)

[43] Ricci ML, Rota MC, Scaturro M, Nardone M, Veschetti E, Lucentini L, Bonadonna L, La Mura S., per la prevenzione del rischio Legionella nei riuniti odontoiatrici durante la pandemia da COVID-19. Versione del 17 maggio 2020. Roma: Istituto Superiore di Sanità; 2020. (Rapporto ISS COVID-19, n. 27/2020).

[44] Gruppo di Lavoro ISS Test Diagnostici COVID-19 e Gruppo di Lavoro ISS Dispositivi Medici COVID-19, *Dispositivi diagnostici in vitro per COVID-19. Parte 1: normativa e tipologie.* Versione del 18 maggio 2020. Roma: Istituto Superiore di Sanità; 2020. (Rapporto ISS COVID-19 n. 28/2020)

[45] Gruppo di lavoro ISS Malattie Rare COVID-19,*Indicazioni ad interim su malattia di Kawasaki e sindrome infiammatoria acuta multisistemica in età pediatrica e adolescenziale nell'attuale scenario emergenziale da infezione da SARS-CoV-2.* Versione 21 maggio 2020. Roma: Istituto Superiore di Sanità; 2020. (Rapporto ISS COVID-19, n. 29/2020)

[46] Gruppo di lavoro Salute mentale ed emergenza COVID-19. *Indicazioni sull'intervento telefonico di primo livello per l'informazione personalizzata e l'attivazione dell'empowerment della popolazione nell'emergenza COVID-19.* Versione del 14 maggio 2020. Roma: Istituto Superiore di Sanità; 2020. (Rapporto ISS COVID-19 n. 30/2020)

[47] Gruppo di lavoro Salute mentale ed emergenza COVID-19. *Indicazioni ad interim per il supporto psicologico telefonico di secondo livello in ambito sanitario*

nello scenario emergenziale COVID-19. Versione del 26 maggio 2020. Roma: Istituto Superiore di Sanità; 2020. (Rapporto ISS COVID-19 n. 31/2020)

[48] L. Boltzmann, Sitz. Akad. Wiss. Wienn 66 275. 1872.

[49] G. Spiga, T. Nonnenmacher and V. C. Boffi, *Moment equations for the diffusion of the particles of a mixture via the scattering kernel formulation of the nonlinear Boltzmann equation.* Physica A, **131**: 431-448, 1985.

[50] V. C. Boffi, V. Protopopescu and G. Spiga, *On the equivalence between the probabilistic, kinetic, and scattering kernel formulations of the Boltzmann equation.* Physica A, **164**: 400-410, 1990.

[51] M. Delitala, *Generalized kinetic theory approach to modeling spread and evolution of epidemics.* Mathematical and Computer Modelling, **39**: 1-12, 2004.

[52] S. De Lillo, M. Delitala and M. C. Salvatori, *Modelling epidemics and virus mutations by methods of the mathematical kinetic theory for active particles.* Mathematical Models and Methods in Applied Sciences, **19**: 1405-1425, 2009.

[53] A. Rossani and G. Spiga, *A note on the kinetic theory of chemically reacting gases.* Physica A, **272**: 563-573, 1999.

[54] A. Belloquid and M. Delitala, *Modeling complex biological system: A kinetic theory approach.* Birkhauser, 2006.

[55] European Centre for Disease Prevention and Control, *Point prevalence survey of healthcare associated infections and antimicrobial use in European acute care hospitals.* 2013.

[56] M. Monaco, T. Giani, M. Raffone, F. Arena, A. Garcia-Fernandez, S. Pollini; Network EuSCAPE-Italy, H. Grundmann, A. Pantosti, G. Rossolini, *Colistin resistance superimposed to endemic carbapenem-resistant Klebsiella pneumoniae: a rapidly evolving problem in Italy.* Euro Surveill. 2014.

[57] GiViTI. *Rapporto progetto PROSAFE - Petalo Infezioni.* Ranica (BG), 2016.

[58] Mortari L. Decidere in Terapia Intensiva. Una ricerca fenomenologica. Volume 1 - Il campo di Firenze. 2014, Verona: QuiEdit editore. ISBN: 9788864642819

[59] S. Finazzi, G. Mandelli, E. Garbero, M. Mondini, G. Trussardi, M. Giardino, M. Tavola, and G. Bertolini, *Data collection and research with MargheritaTre.* Physiological measurement, IOP Publishing, **39**: 2018.

[60] Guest GS, MacQueen KM, Namey EE, *Applied thematic analysis.* Los Angeles, US: SAGE Publications, 2012.

[61] Denis Kuperberg, Damien Pous, and Pierre Pradic, *Kleene Algebra with Hypotheses Amina Doumane.* Univ. Lyon, EnsL, UCBL, CNRS, LIP, 69342 Lyon Cedex, France, 2007.

[62] Christopher Z. Mooney, *Monte Carlo Simulation.* Sage University Paper series on Quantitative Applications in Social Sciences. 1997.

[63] Krishnamurty Muralidhar, *Monte Carlo Simulation.* Encyclopedia of Information Systems. 193-201: 2003.

[64] Peter L. Bonate, *A Brief Introduction to Monte Carlo Simulation.* 2001. DOI: 10.2165/00003088-200140010-00002 ·

[65] Michael R. Chernick *Bootstrap Methods: A Guide for Practitioners and Researchers.* United BioSource Corporation Newtown, PA. 2007.

[66] J. J. Anagnost and C. A. Desoe, *An elementary proof of the Routh-Hurwitz Stability Criterion* VOL. 10, NO. 1, 1991

List of Figures

List of Tables